R. & M. No. 3052
(17,750)
A.R.C. Technical Report

MINISTRY OF SUPPLY

AERONAUTICAL RESEARCH COUNCIL
REPORTS AND MEMORANDA

On the Stressing of Multi-Rib Thin Wings of Low Aspect Ratio and Rectangular Plan-form

By

L. S. D. MORLEY

LONDON : HER MAJESTY'S STATIONERY OFFICE
1958

SIXTEEN SHILLINGS NET

On the Stressing of Multi-Rib Thin Wings of Low Aspect Ratio and Rectangular Plan-form

By

L. S. D. Morley

Communicated by the Principal Director of Scientific Research (Air), Ministry of Supply

Reports and Memoranda No. 3052*

January, 1955

Summary.—Exact theories are used to examine the validity of certain methods of wing stressing when they are applied to thin wings of low aspect ratio. Attention is confined to the two spar multi-rib wing having rectangular cross-section and rectangular plan-form.

1. *Introduction.*—In certain methods of wing stressing[1, 2], hereafter referred to as conventional, no account is taken of :

(*a*) the chordwise distribution of loading

(*b*) the cross-sectional distortion of the ribs (apart from pure shear)

(*c*) the exact elastic behaviour of the top and bottom skins

and these effects become important as the wing thickness and aspect ratio decrease.

In this paper, attention is confined to the two-spar multi-rib wing having rectangular cross-section and rectangular plan-form. The exact equations of elasticity are derived and solved, and numerical examples are given for a thin wing of low aspect ratio. These results are compared with those obtained from the conventional methods[1, 2].

The loading on such wings can always be separated into loadings symmetrical and anti-symmetrical about the spanwise centre-line of the wing box. The problems associated with each type of loading are respectively examined under the general headings of the 'Flexural' and 'Torsional' cases. For the 'Torsional' case a simplified analysis is also given and this yields a better approximation than the conventional method[2]. The important case of loading along one spar is also discussed.

2. *Description of Structure and Assumptions.*—The top and bottom surfaces of the two-spar multi-rib wing of rectangular cross-section and rectangular plan-form, shown in Fig. 1, are constructed from thin flat skins reinforced by closely spaced stringers and rib booms. The spar and rib webs are reinforced by closely spaced inextensional members parallel to the z-axis. The wing is supported mid-way along each spar and these supports supply z-wise constraint only.

*R.A.E. Report Structures 171, received 14th July, 1955.

The following assumptions are made in the analysis :

(a) The stress-strain relationships are linear

(b) Buckling does not occur

(c) The stringers and booms resist only direct load

(d) The stringers and ribs are so closely spaced that they may be considered uniformly distributed

(e) The spar and rib webs resist only shear, account being taken of their contribution to the direct stiffnesses by corresponding increases in the spar-boom and rib-boom cross-sections.

3. *The Flexural Case.*—The flexural case corresponds to a loading symmetrically distributed about the spanwise centre-line of the wing box. For such loadings the spar and rib web shears are statically determinate and so the three-dimensional problem is reduced to a plane problem where all the boundary conditions are known.

The equations of compatibility for the reinforced skins at $z = \pm b$ are derived in terms of the displacements u and v in Appendix I.

They are

$$\left.\begin{aligned} &\alpha^* \left(\frac{a}{L}\right)^2 \frac{\partial^2 u}{\partial \xi^2} + \frac{1-\sigma}{2} \frac{\partial^2 u}{\partial \eta^2} = -\frac{1+\sigma}{2}\left(\frac{a}{L}\right) \frac{\partial^2 v}{\partial \xi\, \partial \eta} \\ &\bar{\alpha} \frac{\partial^2 v}{\partial \eta^2} + \frac{1-\sigma}{2}\left(\frac{a}{L}\right)^2 \frac{\partial^2 v}{\partial \xi^2} = -\frac{1+\sigma}{2}\left(\frac{a}{L}\right) \frac{\partial^2 u}{\partial \xi\, \partial \eta} + \frac{1-\sigma^2}{Et} a^2 \bar{S} \end{aligned}\right\}, \quad \ldots \quad (1)$$

where α^* and $\bar{\alpha}$ are non-dimensional structural constants and $\bar{S}$ is the known surface force applied by the rib webs. The remainder of the notation is defined in Fig. 1. Equations (1) are solved in Appendix II for the particular loading cases of

(a) uniformly distributed load over the whole surface, *i.e.*, $Z(\xi, \eta) = Z =$ a constant

(b) uniformly distributed load along the two spars, *i.e.*, $Z_R(\xi) = Z_R =$ a constant.

The solutions are :

$$\left.\begin{aligned} u = {} & \frac{1-\sigma^2}{Et} \sum_{n=1}^{\infty} \sin \frac{n\pi\xi}{2} \left\{ A_{1n} \cosh \frac{n\pi\beta_1^{-1/2}\eta}{2} + A_{2n} \cosh \frac{n\pi\beta_2^{-1/2}\eta}{2} \right\} \\ & + \frac{1-\sigma^2}{Et} \sum_{m=1}^{\infty} \cos \frac{m\pi\eta}{2} \left\{ B_{1m} \sinh \frac{m\pi\beta_1^{1/2}\xi}{2} + B_{2m} \sinh \frac{m\pi\beta_2^{1/2}\xi}{2} \right\} \\ v = {} & \frac{1-\sigma^2}{Et} (2aLZ) \left(\frac{a^2}{bL}\right) \frac{1}{8\bar{\alpha}} \left(\frac{\eta^3}{3} - \eta\right) - \frac{1-\sigma^2}{Et} \sum_{n=1}^{\infty} \cos \frac{n\pi\xi}{2} \\ & \left\{ \lambda_1 A_{1n} \sinh \frac{n\pi\beta_1^{-1/2}\eta}{2} + \lambda_2 A_{2n} \sinh \frac{n\pi\beta_2^{-1/2}\eta}{2} \right\} \\ & - \frac{1-\sigma^2}{Et} \sum_{m=1}^{\infty} \sin \frac{m\pi\eta}{2} \left\{ \lambda_1 B_{1m} \cosh \frac{m\pi\beta_1^{1/2}\xi}{2} + \lambda_2 B_{2m} \cosh \frac{m\pi\beta_2^{1/2}\xi}{2} \right\} \end{aligned}\right\} \quad \ldots \quad (2)$$

where β_1, β_2, λ_1, λ_2 are non-dimensional structural constants, n, m are odd integers and A_{1n}, A_{2n}, B_{1m}, B_{2m} are arbitrary constants to be determined from the boundary conditions. The determination of the arbitrary constants involves the solution of four sets of infinite simultaneous equations but the form of equations (2) has been chosen so that these equations readily reduce to a single set of infinite simultaneous equations where the leading diagonal terms are predominant.

When the arbitrary constants have been determined, the stress distribution throughout the wing is evaluated, using the well-known stress-strain relationships, and the distortion of the wing is evaluated from the expression

$$\bar{w}(\xi, \eta) = -\frac{2(1+\sigma)}{E\tau} a \int_{\eta}^{1} \bar{S}\, d\eta + \frac{a}{b}\int_{\eta}^{1} v\, d\eta + \frac{2(1+\sigma)}{Et_R} L \int_{0}^{\xi} S_R\, d\xi - \frac{L}{b}\int_{0}^{\xi} u/_{\eta=1}\, d\xi \quad \ldots \quad (3)$$

where $\bar{w}(\xi, \eta)$ is the z-wise displacement.

If the ribs are assumed rigid in their own plane there is a considerable simplification in the analysis and computation. This simplification is considered in Appendix III and corresponds to the conventional method[1] of stressing for the flexural case. The equation of compatibility for the reinforced skins at $z = \pm b$ is then

$$\beta \frac{\partial^2 u}{\partial \xi^2} + \frac{\partial^2 u}{\partial \eta^2} = 0 \quad \ldots \quad (4)$$

and the solution is simply

$$\left.\begin{aligned} u &= \frac{1}{Et}\sum_{n=1}^{\infty} A_n \sin\frac{n\pi\xi}{2}\cosh\frac{n\pi\beta^{1/2}\eta}{2} \\ v &= 0 \end{aligned}\right\}, \quad \ldots \quad (5)$$

where β is a non-dimensional structural constant, n is an odd integer and the A_n are arbitrary constants to be determined from a boundary condition.

A numerical illustrative example is given in Appendix V and is based on a wing whose structural box has an aspect ratio 2 and a thickness/chord ratio 7·5 per cent. The stress distributions for this wing are shown in Figs. 6 to 15 and the distorted shape is shown in Figs. 16 and 17. For the purpose of ready comparison the salient values are reproduced in the table.

The additional effects due to the chordwise distribution of loading may be approximated by the simplified method given in Appendix VI. Appendix VII deals briefly with the anti-clastic effects due to pure bending.

4. *The Torsional Case.*—The torsional case corresponds to a loading anti-symmetrically distributed about the spanwise centre-line of the wing box. Unlike the flexural case, the spar and rib web shears are no longer statically determinate and so the problem is three-dimensional. The analysis could proceed in a similar manner as for the flexural case, but as the algebra and computation would be more intricate a different approach has been favoured (Appendix VIII).

The equations of equilibrium for the reinforced skins at $z = \pm b$ are

$$\left.\begin{aligned} \left(\frac{a}{L}\right)\frac{\partial T}{\partial \xi} + \frac{\partial S}{\partial \eta} &= 0 \\ \left(\frac{a}{L}\right)\frac{\partial S}{\partial \xi} + \frac{\partial T'}{\partial \eta} - a\bar{S} &= 0 \\ \bar{S} &= \frac{1}{L}\frac{d}{d\xi}\int_{0}^{1} S\, d\eta \end{aligned}\right\}, \quad \ldots \quad (6)$$

	Uniformly distributed load over whole surface $2aLZ = 1\cdot 0$ lb	Uniformly distributed load along the spars, $2LZ_R = 1\cdot 0$ lb	Rigid ribs, $2LZ_R = 1\cdot 0$ lb. Conventional method	Engineer's bending theory $2LZ_R = 1\cdot 0$ lb	Statically zero distributed load $2aLZ - 2LZ_R$	Statically zero distributed load $2aLZ - 2LZ_R$ acting on a wing of infinite span	Anti-clastic effects due to a tip moment $L^2Z_R = L/2$ in. lb
Max. spar boom stress (*i.e.*, at $\xi = 0$, $\eta = 1$)	0·2036 lb/in.²	0·1999 lb/in.²	0·1955 lb/in.²	0·1111 lb/in.²	0·0037 lb/in.²	0·0047 lb/in.²	0·1111 lb/in.²
Max. spanwise skin stress (*i.e.*, at $\xi = 0$, $\eta = 1$)	0·2067 lb/in.²	0·2032 lb/in.²	0·1955 lb/in.²	0·1111 lb/in.²			0·1111 lb/in.²
Max. rib-boom stress at tip (*i.e.*, at $\xi = 1$, $\eta = 0$)	—0·0953 lb/in.²	—0·0573 lb/in.²	0	0	—0·0380 lb/in.²	—0·0440 lb/in.²	
Max. chordwise skin stress at tip (*i.e.*, at $\xi = 1$, $\eta = 0$)	—0·0974 lb/in.²	—0·0586 lb/in.²	0	0			
z-wise deflection of spar at tip	$-2\cdot795 \times 10^{-5}$ in.	$-2\cdot716 \times 10^{-5}$ in.	$-2\cdot622 \times 10^{-5}$ in.	$-1\cdot481 \times 10^{-5}$ in.			
z-wise deflection at centre of tip rib	$-3\cdot360 \times 10^{-5}$ in.	$-3\cdot047 \times 10^{-5}$ in.	$-2\cdot622 \times 10^{-5}$ in.	$-1\cdot481 \times 10^{-5}$ in.	$-0\cdot313 \times 10^{-5}$ in.	$-0\cdot273 \times 10^{-5}$ in.	
z-wise deflection at centre of root rib	$-0\cdot174 \times 10^{-5}$ in.	$0\cdot105 \times 10^{-5}$ in.	0	0	$-0\cdot279 \times 10^{-5}$ in.	$-0\cdot273 \times 10^{-5}$ in.	$-0\cdot186 \times 10^{-5}$ in.

The values of the structural constants are:

a	=	100 in.	Semi-chord dimension
A	=	10 in.²	Cross-sectional area of the front and rear spar booms
b	=	7·5 in.	Semi-spar depth
L	=	200 in.	Semi-span dimension
t	=	0·15 in.	Nominal thickness of top and bottom skins
t_R	=	0·15 in.	Nominal thickness of the front and rear spar webs
t^*	=	0·20 in.	Effective thickness of the skin-stringer combination for resisting load in the direction of the stringers
$\bar{t}$	=	0·18 in.	Effective thickness of the skin-rib boom combination for resisting load in the direction of the ribs
τ	=	0·008	Thickness of rib webs per unit length of span

where T, T' and S are stress resultants. A consistent system of stress resultants satisfying these equations is then

$$\left.\begin{aligned} T &= \sum_{n=1}^{\infty} \eta^n F_n(\xi) \\ T' &= -\left(\frac{a}{L}\right)^2 \frac{d^2}{d\xi^2} \sum_{n=1}^{\infty} \frac{\eta(1-\eta^{n+1})}{(n+1)(n+2)} F_n(\xi) \\ S &= -\left(\frac{a}{L}\right) \frac{d}{d\xi} \left\{F(\xi) + \sum_{n=1}^{\infty} \frac{\eta^{n+1}}{n+1} F_n(\xi)\right\} \\ \bar{S} &= -\frac{1}{L}\left(\frac{a}{L}\right) \frac{d^2}{d\xi^2} \left\{F(\xi) + \sum_{n=1}^{\infty} \frac{1}{(n+1)(n+2)} F_n(\xi)\right. \end{aligned}\right\} \quad \ldots \quad \ldots \quad (7)$$

where n is an odd integer and $F(\xi)$, $F_n(\xi)$ are functions to be determined from the condition that the total strain energy is a minimum. This procedure yields $(n + 3)/2$ simultaneous differential equations of fourth order involving only the even differentials. The arbitrary constants in the complementary functions are determined from the boundary conditions at $\xi = 0$ and $\xi = 1$, which yield two sets of $n + 3$ simultaneous equations.

When these functions have been determined, the stress distribution throughout the wing is evaluated by substitution into equations (7) and others, and the distortion of the wing is evaluated from the expression

$$\bar{w}(\xi, \eta) = \frac{2(1+\sigma)}{E\tau} a \int_0^\eta \bar{S}\, d\eta - \frac{a}{b} \int_0^\eta v\, d\eta \,. \quad \ldots \quad \ldots \quad \ldots \quad \ldots \quad \ldots \quad (8)$$

It should be noted that the above procedure corresponds to the conventional[2] method when the $F_n(\xi)$ are put equal to zero.

Since the effect of the chordwise distribution of loading will, in general, be smaller than for the flexural case, the equations have been solved only for a uniformly distributed load along each spar, *viz.*, $2LZ_R = 1 \cdot 0$ lb. Numerical illustrative examples are given in Appendix X for the same wing examined for the flexural case.

The determination of the cross-sectional distortion is unlikely to be of such importance as for the flexural case since the distortion will be of a smaller order due to the presence of a point of inflexion along the spanwise centre-line. This suggests that the rib booms might be considered inextensional, thereby simplifying the analysis. This simplification is considered in Appendix IX where the equations of compatibility are found to be

$$\left.\begin{aligned} &\beta \frac{\partial^2 u}{\partial \xi^2} + \frac{\partial^2 u}{\partial \eta^2} = 0 \\ &\frac{1}{\tau}\left(\frac{ab}{L^2}\right)\frac{d^3 v}{d\xi^3} - \left(\frac{a}{t} + \frac{b}{t_R}\right)\frac{dv}{d\xi} = -\left(\frac{L}{a}\right)\left(\frac{a}{t} - \frac{b}{t_R}\right)u\Big/_{\eta=1} - \frac{1}{\tau}\left(\frac{b}{L}\right)\frac{\partial^2 u}{\partial \xi^2}\Big/_{\eta=1} \\ &\qquad - \frac{2(1+\sigma)}{Et_R}(2LZ_R)\frac{1}{4}\left(\frac{L}{t}\right)(1-\xi) \end{aligned}\right\} \quad \ldots \quad (9)$$

The solution of these equations is

$$\left.\begin{aligned} u &= \frac{1}{Et}\sum_{n=1}^{\infty} A_n \sin\frac{n\pi\xi}{2}\sinh\frac{n\pi\beta^{1/2}\eta}{2}, \\ \frac{dv}{d\xi} &= \frac{1}{Et}\left(\frac{L}{a}\right)\left\{C_1\sinh\gamma^{1/2}\xi + C_2\cosh\gamma^{1/2}\xi\right. \\ &\quad \left. + \sum_{n=1}^{\infty}\nu_n A_n \sin\frac{n\pi\xi}{2}\sinh\frac{n\pi\beta^{1/2}}{2}\right\} \\ &\quad + \frac{2(1+\sigma)}{Et_R}\left(\frac{L}{t}\right)(2LZ_R)\frac{(1-\xi)}{4\left(\dfrac{a}{t}+\dfrac{b}{t_R}\right)} \end{aligned}\right\}, \qquad \ldots \quad \ldots \quad \ldots \quad (10)$$

where γ and ν_n are non-dimensional structural constants, n is an odd integer and C_1, C_2 and A_n are arbitrary constants to be determined from the boundary conditions. A numerical illustrative example is given in Appendix X.

The stress distributions obtained from the various numerical examples are shown in Figs. 18 to 22 and the spar deflections are shown in Fig. 23. For the purpose of ready comparison, the salient values are reproduced in the table, where the loading for all cases is uniformly distributed along each spar and of magnitude $2LZ_R = 1\cdot 0$ lb.

5. *Loading Along one Spar.*—For an aircraft in subsonic flight the lift distribution is usually such that the centre of pressure is in the neighbourhood of the front spar. An important design case therefore occurs where the structural box is loaded along one spar only. The stress and distorted shape for this loading can be easily obtained by addition of the results of the flexural and torsional cases ; the results of this addition are shown in Fig. 24 for the spar boom stresses.

The increase in maximum spar boom stress over that given by the conventional methods is approximately 10 per cent for the wing investigated. It is to be expected that this difference will increase as the thickness and aspect ratio of the structural box decrease.

6. *Conclusions.*—The validity of the conventional methods of wing stressing[1, 2] has been examined when they are applied to thin wings of low aspect ratio. Attention has been confined to the two-spar multi-rib wing having rectangular cross-section and rectangular plan-form.

For loadings symmetrical about the spanwise centre-line of the wing box (the flexural case) it has been found from a numerical comparison that the conventional method[1] is satisfactory in all respects excepting that it does not reveal

(*a*) the cross-sectional distortion of the ribs (*i.e.*, the change in camber)

(*b*) the chordwise stresses in the reinforced skins.

The conventional method[2] of wing stressing for loadings anti-symmetrical about the spanwise centre-line (the torsional case) is not satisfactory and yields optimistic results. The use of an 'effective' boom area including 1/6 of the cross-sectional area of the reinforced skin is less accurate than using the nominal boom area for these thin wings. An exact and a simplified analysis are given in the Appendices.

Uniformly distributed Load $2LZ_R = 1 \cdot 0$ *lb. along each Spar*

	Appendix VIII First two terms	Appendix VIII First term with nominal spar boom area	Appendix VIII First term with effective† spar boom area. Conventional method	Appendix VIII First term with effective† spar boom area and rigid ribs	Appendix IX Inextensional rib booms
Max. spar-boom stress (*i.e.*, at $\xi = 0$, $\eta = 1$)	0·1275 lb/in.^{2}	0·1424 lb/in.^{2}	0·1000 lb/in.^{2}	0·0953 lb/in.^{2}	0·1232 lb/in.^{2}
Max. skin shear stress	0·0582 lb/in.^{2}	0·0418 lb/in.^{2}	0·0360 lb/in.^{2}	0·0351 lb/in.^{2}	0·0520 lb/in.^{2}
Max. spar-web shear stress	−0·222 lb/in.^{2}	−0·222 lb/in.^{2}	−0·222 lb/in.^{2}	−0·207 lb/in.^{2}	−0·222 lb/in.^{2}
z-wise deflection of spar at tip	$-1 \cdot 324 \times 10^{-5}$ in.	$-1 \cdot 402 \times 10^{-5}$ in.	$-1 \cdot 271 \times 10^{-5}$ in.	$-1 \cdot 222 \times 10^{-5}$ in.	$-1 \cdot 279 \times 10^{-5}$ in.

† Effective spar boom area $= A + at^*/3$

The values of the structural constants are :

a	=	100 in.	Semi-chord dimension
A	=	10 in.^{2}	Cross-sectional area of the front and rear spar booms
b	=	7·5 in.	Semi-spar depth
L	=	200 in.	Semi-span dimension
t	=	0·15 in.	Nominal thickness of top and bottom skins
t_R	=	0·15 in.	Nominal thickness of the front and rear spar webs
t^*	=	0·20 in.	Effective thickness of the skin-stringer combination for resisting load in the direction of the stringers
$\bar{t}$	=	0·18 in.	Effective thickness of the skin-rib boom combination for resisting load in the direction of the ribs
τ	=	0·008	Thickness of rib webs per unit length of span

LIST OF SYMBOLS

1. *General*.—1.1. *Structural Properties*

$2a$	Chord of the wing structure
A	Cross-sectional area of the front and rear spar booms
$2b$	Thickness of the wing structure
$2L$	Span of the wing structure
t	Nominal thickness of the top and bottom skins
t_R	Nominal thickness of the front and rear spar webs
t^*	Effective thickness of the skin–stringer combination for resisting load in the direction of the stringers
$\bar{t}$	Effective thickness of the skin–rib-boom combination for resisting load in the direction of the ribs
τ	Thickness of rib webs per unit length of span

1.2. *Co-ordinate Systems*

x, y, z	Rectangular co-ordinate system with origin at centre of wing
ξ	$= x/L$ Non-dimensional co-ordinate
η	$= y/a$ Non-dimensional co-ordinate

1.3. *Loads and Stresses*

P_R	End load in the rear spar boom
S	Shear-stress resultant in the reinforced skin
S_R	Shear-stress resultant in the rear spar web
$\bar{S}$	Surface force acting on the skin
T	Direct-stress resultant in the reinforced skin along a stringer
T'	Direct-stress resultant in the reinforced skin along a rib boom
$Z(\xi, \eta)$	Distributed load acting over the whole wing
Z	Uniformly distributed load acting on the whole wing
$Z_R(\xi)$	Distributed load acting on the rear spar
Z_R	Uniformly distributed load acting on the rear spar

1.4. *Displacements*

u	Displacement along a stringer
u_R	Displacement along a spar boom
u_R'	x-wise displacement in a spar web
v	Displacement along a rib boom
$\bar{v}$	y-wise displacement in a rib web
$\bar{w}$	z-wise displacement in a rib
$\bar{w}_0$	z-wise displacement of the centre of a rib
w_R	z-wise displacement of a spar

1.5. *Elastic Constants*

E	Young's modulus of elasticity for the structure
σ	Poisson's ratio for the structure

2. *Symbols Peculiar to Appendices I, II and V.*

$A_{1n}, A_{2n}, B_{1m}, B_{2m}$	Arbitrary constants
n, m	Odd integers

$$\left.\begin{aligned} \alpha^* &= \frac{t^*}{t} - \sigma^2\left(\frac{t^*}{t} - 1\right) \\ \bar{a} &= \frac{\bar{t}}{t} - \sigma^2\left(\frac{\bar{t}}{t} - 1\right) \end{aligned}\right\} \text{non-dimensional structural parameters}$$

$$\left.\begin{aligned} \beta_1\beta_2 &= \left(\frac{L}{a}\right)^4 \frac{\bar{a}}{\alpha^*} \\ \beta_1 + \beta_2 &= \left(\frac{L}{a}\right)^2 \frac{2(\alpha^*\bar{a} - \sigma)}{\alpha^*(1 - \sigma)} \\ \lambda_1 &= \frac{2\alpha^*}{1 + \sigma}\left(\frac{a}{L}\right)\beta_1^{1/2} - \frac{1 - \sigma}{1 + \sigma}\left(\frac{L}{a}\right)\beta_1^{-1/2} \\ \lambda_2 &= \frac{2\alpha^*}{1 + \sigma}\left(\frac{a}{L}\right)\beta_2^{1/2} - \frac{1 - \sigma}{1 + \sigma}\left(\frac{L}{a}\right)\beta_2^{-1/2} \end{aligned}\right\} \text{non-dimensional structural parameters}$$

3. *Symbols Peculiar to Appendices IV and IX.*

A_n	Arbitrary constant
C_1, C_2	Arbitrary constants
n	Odd integer

$$\left.\begin{aligned} \beta &= \left(\frac{a}{L}\right)^2 2(1 + \sigma)\frac{t^*}{t} \\ \gamma &= \left(\frac{L^2}{ab}\right)\tau\left(\frac{a}{t} + \frac{b}{t_R}\right) \end{aligned}\right\} \text{non-dimensional structural parameters}$$

$\theta_n, \nu_n, \rho_n, \varphi_n, \psi_n$ = constants defined in Appendix IX

4. *Symbols Peculiar to Appendix VIII.*

A_e	Effective cross-sectional area of the front and rear spar booms
	$= A + at^*/3$
F, F_n	Functions of ξ defining the stress distribution
n	Odd integer
δ	Infinitesimal variation

REFERENCES

No.	Author	Title, etc.
1	D. Williams, R. D. Starkey and A. H. Taylor ..	Distribution of stress between spar flanges and stringers for a wing under distributed loading. R. & M. 2098. June, 1939.
2	H. L. Cox	On the stressing of polygonal tubes with particular reference to the torsion of tapered tubes of trapezoidal section. R. & M. 1908, December, 1942.

APPENDIX I

The Flexural Case

Derivation of Fundamental Equations

The flexural case corresponds to a loading symmetrically distributed about the spanwise centre-line of the wing box. For such loadings the spar and rib-web shears are statically determinate and so the three-dimensional problem is reduced to a plane problem where all the boundary conditions are known. In what follows, attention is confined to cases where the displacements u and v at $z = \pm b$ are equal and opposite to one another.

1. *Fundamental Equations for the Reinforced Skins $z = \pm b$.*—For equilibrium of an elemental portion of the reinforced skin at $z = b$, Fig. 2, it is necessary that

$$\left.\begin{aligned} \left(\frac{a}{L}\right)\frac{\partial T}{\partial \xi} + \frac{\partial S}{\partial \eta} &= 0 \\ \left(\frac{a}{L}\right)\frac{\partial S}{\partial \xi} + \frac{\partial T'}{\partial \eta} - a\bar{S} &= 0 \end{aligned}\right\} \quad \ldots \quad (11)$$

The stress resultants in terms of the displacements are

$$\left.\begin{aligned} T &= \frac{Et}{1-\sigma^2}\left(\frac{\alpha^*}{L}\frac{\partial u}{\partial \xi} + \frac{\sigma}{a}\frac{\partial v}{\partial \eta}\right) \\ T' &= \frac{Et}{1-\sigma^2}\left(\frac{\bar{a}}{a}\frac{\partial v}{\partial \eta} + \frac{\sigma}{L}\frac{\partial u}{\partial \xi}\right) \\ S &= \frac{Et}{2(1+\sigma)}\left(\frac{1}{a}\frac{\partial u}{\partial \eta} + \frac{1}{L}\frac{\partial v}{\partial \xi}\right) \end{aligned}\right\}, \quad \ldots \quad (12)$$

where α^* and $\bar{a}$ are non-dimensional structural constants given by

$$\alpha^* = \frac{t^*}{t} - \sigma^2\left(\frac{t^*}{t} - 1\right);$$

$$\bar{a} = \frac{\bar{t}}{t} - \sigma^2\left(\frac{\bar{t}}{t} - 1\right).$$

The equations of equilibrium in terms of the displacements are then found to be

$$\left.\begin{aligned} \alpha^*\left(\frac{a}{L}\right)^2\frac{\partial^2 u}{\partial \xi^2} + \frac{1-\sigma}{2}\frac{\partial^2 u}{\partial \eta^2} &= -\frac{1+\sigma}{2}\left(\frac{a}{L}\right)\frac{\partial^2 v}{\partial \xi\,\partial \eta} \\ \bar{a}\,\frac{\partial^2 v}{\partial \eta^2} + \frac{1-\sigma}{2}\left(\frac{a}{L}\right)^2\frac{\partial^2 v}{\partial \xi^2} &= -\frac{1+\sigma}{2}\left(\frac{a}{L}\right)\frac{\partial^2 u}{\partial \xi\,\partial \eta} + \frac{1-\sigma^2}{Et}\,a^2\bar{S} \end{aligned}\right\} \quad \text{or (1) bis.} \qquad (13)$$

2. *Fundamental Equations for the Spar Booms.*—The spar booms are additional end-load carrying members attached along the outer edges of the reinforced skin. The forces acting on an elemental portion of the rear spar boom are shown in Fig. 3. For equilibrium of this element it is necessary that

$$\frac{1}{L}\frac{dP_R}{d\xi} = S_R + S/_{\eta=1},$$

which on integration yields

$$P_R = -L\int_\xi^1 (S_R + S/_{\eta=1})\,d\xi \qquad (14)$$

where it is assumed that $P_R = 0$ at the tip.

The condition of compatibility between the rear spar boom and adjacent reinforced skin is that

$$\frac{du_R}{d\xi} = \frac{\partial u}{\partial \xi}\Big/_{\eta=1}, \qquad (15)$$

where the boom strain is

$$\frac{du_R}{d\xi} = -\frac{L^2}{EA}\int_\xi^1 (S_R + S/_{\eta=1})\,d\xi\,. \qquad (16)$$

3. *Fundamental Equations for the Ribs and Spar Webs.*—The forces acting on a rib are shown in Fig. 4. The ribs are continuously distributed in the ξ direction and the thickness of rib webs within an element $L\delta\xi$ will be denoted $\tau L\,\delta\xi$. The shear stress resultant acting on a rib is denoted by $\bar{S}L\,\delta\xi$ where the stress $\bar{S}$ is, in general, a function of ξ and η. For equilibrium of a rib it is necessary that

$$\frac{\partial \bar{S}}{\partial \eta} = \frac{aZ(\xi, \eta)}{2b}, \qquad (17)$$

where $Z(\xi, \eta)$ is the distributed load over the wing surface. The relation between $\bar{S}$ and the rib displacements is

$$\frac{1}{a}\frac{\partial \bar{w}}{\partial \eta} + \frac{\partial \bar{v}}{\partial z} = \frac{2(1+\sigma)}{E\tau}\,\bar{S}\,.$$

Now, the ribs are reinforced by inextensional z-wise members and so it follows that $\bar{w}$ is independent of z. Differentiation of this equation with respect to z then shows that

$$\bar{v} = \frac{z}{b}\,v\,,$$

since at $z = \pm b$ the rib displacements must conform with those of the reinforced skin. It now follows that

$$\bar{w} = \frac{2(1+\sigma)}{E\tau}\,a\int_0^\eta \bar{S}\,d\eta - \frac{a}{b}\int_0^\eta v\,d\eta + \bar{w}_0 \qquad (18)$$

where $\bar{w}_0 = \bar{w}/_{\eta=0}$ and is a function only of ξ.

The forces acting on the rear spar web are shown in Fig. 5. For equilibrium at the intersection of the rib and spar webs it is necessary that

$$\frac{1}{L}\frac{dS_R}{d\xi} - \bar{S}/_{\eta=1} = \frac{Z_R(\xi)}{2b}, \quad \ldots \quad (19)$$

where $Z_R(\xi)$ is the distributed load along the rear spar. The relation between S_R and the spar displacements is

$$\frac{1}{L}\frac{\partial w_R}{\partial \xi} + \frac{\partial u'_R}{\partial z} = \frac{2(1+\sigma)}{Et_R} S_R .$$

Differentiation of this equation with respect to z then shows that

$$u_R' = \frac{z}{b} u/_{\eta=1}$$

since at $z = \pm b$ the spar-web displacements must agree with those of the spar boom, and because agreement of the z-wise displacement w_R with the displacement $\bar{w}$ shows that the former are also independent of the z co-ordinate. This and the strain equation then yield

$$w_R = \frac{2(1+\sigma)}{Et_R} L \int_0^{\xi} S_R \, d\xi - \frac{L}{b}\int_0^{\xi} u/_{\eta=1} d\xi , \quad \ldots \quad (20)$$

since at the root $w_{R/\xi=0} = 0$.

Noting that $w_R = \bar{w}/_{\eta=1}$, it is easily shown from equations (18) and (20) that

$$\bar{w}_0 = -\frac{2(1+\sigma)}{E\tau} a \int_0^1 \bar{S}\, d\eta + \frac{a}{b}\int_0^1 v\, d\eta + \frac{2(1+\sigma)}{Et_R} L \int_0^{\xi} S_R\, d\xi - \frac{L}{b}\int_0^{\xi} u/_{\eta=1}\, d\xi .$$

The equation for the rib displacements may now be rewritten

$$\bar{w} = -\frac{2(1+\sigma)}{E\tau} a \int_{\eta}^1 \bar{S}\, d\eta + \frac{a}{b}\int_{\eta}^1 v\, d\eta + \frac{2(1+\sigma)}{Et_R} L \int_0^{\xi} S_R\, d\xi$$

$$- \frac{L}{b}\int_0^{\xi} u/_{\eta=1}\, d\xi \text{ or (3) bis.} \quad \ldots \quad (21)$$

4. *Equation of Overall Equilibrium.*—To complete the formulation it now remains only to determine the equation of overall equilibrium for the wing box. This is determined from resolution of the z-wise forces at a chordwise section, *viz.*,

$$S_R = -\frac{aL}{4b}\int_{-1}^1 \int_{\xi}^1 Z(\xi, \eta)\, d\xi\, d\eta - \frac{L}{2b}\int_{\xi}^1 Z_R(\xi)\, d\xi . \quad \ldots \quad (22)$$

APPENDIX II

The Flexural Case — Solution of Equations

It is now proposed to solve the equations of Appendix I for the particular loading cases of

$$\left.\begin{aligned} Z(\xi, \eta) &= Z = \text{a constant} \\ Z_R(\xi) &= Z_R = \text{a constant} \end{aligned}\right\} \quad \ldots \qquad (23)$$

The equations of equilibrium in terms of the displacements are

$$\left.\begin{aligned} &\alpha^* \left(\frac{a}{L}\right)^2 \frac{\partial^2 u}{\partial \xi^2} + \frac{1-\sigma}{2} \frac{\partial^2 u}{\partial \eta^2} = -\frac{1+\sigma}{2} \left(\frac{a}{L}\right) \frac{\partial^2 v}{\partial \xi \, \partial \eta} \\ &\bar{a} \frac{\partial^2 v}{\partial \eta^2} + \frac{1-\sigma}{2} \left(\frac{a}{L}\right)^2 \frac{\partial^2 v}{\partial \xi^2} = -\frac{1+\sigma}{2} \left(\frac{a}{L}\right) \frac{\partial^2 u}{\partial \xi \, \partial \eta} + \frac{1-\sigma^2}{Et} a^2 \bar{S} \end{aligned}\right\}, \quad (13) \text{ bis}$$

where, from equation (17), the surface force is found to be

$$\bar{S} = \frac{aZ\eta}{2b} \quad \ldots \qquad (24)$$

A solution to equations (13) may be written

$$\left.\begin{aligned} u = {} & \frac{1-\sigma^2}{Et} \sum_{n=1}^{\infty} \sin \frac{n\pi\xi}{2} \left\{ A_{1n} \cosh \frac{n\pi\beta_1^{-1/2}\eta}{2} + A_{2n} \cosh \frac{n\pi\beta_2^{-1/2}\eta}{2} \right\} \\ & + \frac{1-\sigma^2}{Et} \sum_{m=1}^{\infty} \cos \frac{m\pi\eta}{2} \left\{ B_{1m} \sinh \frac{m\pi\beta_1^{1/2}\xi}{2} + B_{2m} \sinh \frac{m\pi\beta_2^{1/2}\xi}{2} \right\} \\ v = {} & \frac{1-\sigma^2}{Et} (2aLZ) \left(\frac{a^2}{bL}\right) \frac{1}{8\bar{a}} \left(\frac{\eta^3}{3} - \eta\right) \\ & - \frac{1-\sigma^2}{Et} \sum_{n=1}^{\infty} \cos \frac{n\pi\xi}{2} \left\{ \lambda_1 A_{1n} \sinh \frac{n\pi\beta_1^{-1/2}\eta}{2} + \lambda_2 A_{2n} \sinh \frac{n\pi\beta_2^{-1/2}\eta}{2} \right\} \\ & - \frac{1-\sigma^2}{Et} \sum_{m=1}^{\infty} \sin \frac{m\pi\xi}{2} \left\{ \lambda_1 B_{1m} \cosh \frac{m\pi\beta_1^{1/2}\xi}{2} + \lambda_2 B_{m2} \cosh \frac{m\pi\beta_2^{1/2}\xi}{2} \right\} \end{aligned}\right\}, (2) \text{ or bis } (25)$$

where n, m are odd integers and

$$\beta_1\beta_2 = \left(\frac{L}{a}\right)^4 \frac{\bar{a}}{\alpha^*},$$

$$\beta_1 + \beta_2 = \left(\frac{L}{a}\right)^2 \frac{2(\alpha^*\bar{a} - \sigma)}{\alpha^*(1-\sigma)},$$

$$\lambda_1 = \frac{2\alpha^*}{1+\sigma} \left(\frac{a}{L}\right) \beta_1^{1/2} - \frac{1-\sigma}{1+\sigma} \left(\frac{L}{a}\right) \beta_1^{-1/2},$$

$$\lambda_2 = \frac{2\alpha^*}{1+\sigma} \left(\frac{a}{L}\right) \beta_2^{1/2} - \frac{1-\sigma}{1+\sigma} \left(\frac{L}{a}\right) \beta_2^{-1/2},$$

and A_{1n}, A_{2n}, B_{1m}, B_{2m} are constants to be determined from the boundary conditions at $\xi = 1$ and $\eta = 1$.

The boundary conditions are :

$$\left.\begin{aligned} T' &= 0 \text{ at } \eta = 1 \\ T &= 0 \text{ at } \xi = 1 \\ S &= 0 \text{ at } \xi = 1 \\ \frac{\partial u}{\partial \xi} &= \frac{du_R}{d\xi} \text{ at } \eta = 1 \end{aligned}\right\} \quad \ldots \quad (26)$$

From equations (12) the first boundary condition requires that

$$\frac{Et}{1-\sigma^2}\left(\frac{\bar{a}}{a}\frac{\partial v}{\partial \eta} + \frac{\sigma}{L}\frac{\partial u}{\partial \xi}\right) = 0 \text{ at } \eta = 1\,,$$

and substituting from equations (25) it is found that

$$\sum_{n=1}^{\infty} \frac{n\pi}{2}\left[\left\{\left(\frac{L}{a}\right)\bar{a}\beta_1^{-1/2}\lambda_1 - \sigma\right\} A_{1n} \cosh\frac{n\pi\beta_1^{-1/2}}{2}\right.$$

$$\left. + \left\{\left(\frac{L}{a}\right)\bar{a}\beta_2^{-1/2}\lambda_2 - \sigma\right\} A_{2n} \cosh\frac{n\pi\beta_2^{-1/2}}{2}\right] \cos\frac{n\pi\xi}{2} = 0\,,$$

and this can only be satisfied if

$$\left\{\left(\frac{L}{a}\right)\bar{a}\beta_1^{-1/2}\lambda_1 - \sigma\right\} A_{1n} \cosh\frac{n\pi\beta_1^{-1/2}}{2}$$

$$+ \left\{\left(\frac{L}{a}\right)\bar{a}\beta_2^{-1/2}\lambda_2 - \sigma\right\} A_{2n} \cosh\frac{n\pi\beta_2^{-1/2}}{2} = 0\,. \quad \ldots \quad (27)$$

The second boundary condition requires that

$$\frac{Et}{1-\sigma^2}\left(\frac{\alpha^*}{L}\frac{\partial u}{\partial \xi} + \frac{\sigma}{a}\frac{\partial v}{\partial \eta}\right) = 0 \text{ at } \xi = 1\,,$$

and substituting from equations (25) it is found that

$$\sum_{m=1}^{\infty} \frac{m\pi}{2}\left[\left\{\left(\frac{a}{L}\right)\alpha^*\beta_1^{1/2} - \lambda_1\sigma\right\} B_{1m} \cosh\frac{m\pi\beta_1^{1/2}}{2}\right.$$

$$\left. + \left\{\left(\frac{a}{L}\right)\alpha^*\beta_2^{1/2} - \lambda_2\sigma\right\} B_{2m} \cosh\frac{m\pi\beta_2^{1/2}}{2}\right] \cos\frac{m\pi\eta}{2} = -(2aLZ)\left(\frac{a^2}{bL}\right)\frac{\sigma}{8\bar{a}}(\eta^2 - 1)$$

whence

$$\left\{\left(\frac{a}{L}\right)\alpha^*\beta_1^{1/2} - \lambda_1\sigma\right\} B_{1m} \cosh\frac{m\pi\beta_1^{1/2}}{2}$$

$$+ \left\{\left(\frac{a}{L}\right)\alpha^*\beta_2^{1/2} - \lambda_2\sigma\right\} B_{2m} \cosh\frac{m\pi\beta_2^{1/2}}{2} = (-)^{(m-1)/2}(2aLZ)\left(\frac{\sigma}{\bar{a}}\right)\left(\frac{a^2}{bL}\right)\frac{8}{m^4\pi^4}\,. \quad (28)$$

The third boundary condition requires that

$$\frac{Et}{2(1+\sigma)}\left(\frac{1}{a}\frac{\partial u}{\partial \eta} + \frac{1}{L}\frac{\partial v}{\partial \xi}\right) = 0 \text{ at } \xi = 1\,,$$

and substituting from equations (25) it is found that

$$\sum_{m=1}^{\infty} \frac{m\pi}{2} \left[\left\{1 + \left(\frac{a}{L}\right)\beta_1^{1/2}\lambda_1\right\}B_{1m} \sinh \frac{m\pi\beta^{1/2}}{2} + \left\{1 + \left(\frac{a}{L}\right)\beta_2^{1/2}\lambda_2\right\}B_{2m} \sinh \frac{m\pi\beta_1^{1/2}}{2}\right] \sin \frac{m\pi n}{2}$$

$$= \left(\frac{a}{L}\right) \sum_{n=1}^{\infty} (-)^{(n-1)/2} \frac{n\pi}{2} \left[\left\{\left(\frac{L}{a}\right)\beta_1^{-1/2} + \lambda_1\right\}A_{1n} \sinh \frac{n\pi\beta_1^{-1/2}\eta}{2}\right.$$

$$\left. + \left\{\left(\frac{L}{a}\right)\beta_2^{-1/2} + \lambda_2\right\}A_{2n} \sinh \frac{n\pi\beta_2^{-1/2}\eta}{2}\right]$$

whence

$$m\pi\left[\left\{1 + \left(\frac{a}{L}\right)\beta_1^{1/2}\lambda_1\right\}B_{1m} \sinh \frac{m\pi\beta_1^{1/2}}{2} + \left\{1 + \left(\frac{a}{L}\right)\beta_2^{1/2}\lambda_2\right\}B_{2m} \sinh \frac{m\pi\beta_2^{1/2}}{2}\right]$$

$$= 4\left(\frac{a}{L}\right) \sum_{n=1}^{\infty} (-)^{(n+m-2)/2} \left[\frac{\left\{\left(\frac{L}{a}\right)\beta_1^{-1/2} + \lambda_1\right\}\beta_1^{-1/2}A_{1n}}{\left(\frac{m}{n}\right)^2 + \beta_1^{-1}} \cosh \frac{n\pi\beta_1^{-1/2}}{2}\right.$$

$$\left. + \frac{\left\{\left(\frac{L}{a}\right)\beta_2^{-1/2} + \lambda_2\right\}\beta_2^{-1/2}A_{2n}}{\left(\frac{m}{n}\right)^2 + \beta_2^{-1}} \cosh \frac{n\pi\beta_2^{-1/2}}{2}\right]. \tag{29}$$

The final boundary condition requires that $\partial u/\partial \xi = du_R/d\xi$ at $\eta = 1$, and substituting from equations (16), (22), (23) and (25) it is found that

$$\frac{1-\sigma^2}{Et} \sum_{n=1}^{\infty} \frac{n\pi}{2} \cos \frac{n\pi\xi}{2} \left[A_{1n} \cosh \frac{n\pi\beta_1^{-1/2}}{2} + A_{2n} \cosh \frac{n\pi\beta_2^{-1/2}}{2}\right]$$

$$= \frac{(2aLZ + 2LZ_R)}{8EAb} L^2(1-\xi)^2 - \frac{1-\sigma^2}{2(1+\sigma)} \frac{L}{EA} \sum_{n=1}^{\infty} \cos \frac{n\pi\xi}{2} \left[\left\{\left(\frac{L}{a}\right)\beta_1^{-1/2} + \lambda_1\right\}A_{1n} \sinh \frac{n\pi\beta_1^{-1/2}}{2}\right.$$

$$\left. + \left\{\left(\frac{L}{a}\right)\beta_2^{-1/2} + \lambda^2\right\}A_{2n} \sinh \frac{n\pi\beta_2^{-1/2}}{2}\right]$$

$$+ \frac{1-\sigma^2}{2(1+\sigma)} \frac{L}{EA} \sum_{n=1}^{\infty} (-)^{(m-1)/2} \left[\left\{\left(\frac{L}{a}\right)\beta_1^{-1/2} + \lambda_1\right\}B_{1m}\left(\cosh \frac{m\pi\beta_1^{1/2}}{2} - \cosh \frac{m\pi\beta_1^{1/2}\xi}{2}\right)\right.$$

$$\left. + \left\{\left(\frac{L}{a}\right)\beta_2^{-1/2} + \lambda_2\right\}B_{2m}\left(\cosh \frac{m\pi\beta_2^{1/2}}{2} - \cosh \frac{m\pi\beta_2^{1/2}\xi}{2}\right)\right],$$

whence

$$A_{1n}\left[n\pi\cosh\frac{n\pi\beta_1^{-1/2}}{2}+\left(\frac{tL}{A}\right)\frac{1}{1+\sigma}\left\{\left(\frac{L}{a}\right)\beta_1^{-1/2}+\lambda_1\right\}\sinh\frac{n\pi\beta_1^{-1/2}}{2}\right]+A_{2n}\left[n\pi\cosh\frac{n\pi\beta_2^{-1/2}}{2}\right.$$

$$\left.+\left(\frac{tL}{A}\right)\frac{1}{1+\sigma}\left\{\left(\frac{L}{a}\right)\beta_2^{-1/2}+\lambda_2\right\}\sinh\frac{n\pi\beta_2^{-1/2}}{2}\right]$$

$$=\frac{4}{1-\sigma^2}\left(\frac{tL}{A}\right)\left(\frac{L}{b}\right)(2aLZ+2LZ_R)\left\{\frac{1}{n^2\pi^2}-\frac{(-)^{(n-1)/2}2}{n^3\pi^3}\right\}+\frac{4}{1+\sigma}\left(\frac{L}{a}\right)\left(\frac{tL}{A}\right)\frac{1}{n\pi}\sum_{m=1}^{\infty}(-)^{(n+m-2)/2}$$

$$\left[\frac{\{(L/a)\beta_1^{-1/2}+\lambda_1\}\beta_1B_{1m}}{(n/m)^2+B_1}\cosh\frac{m\pi\beta_1^{1/2}}{2a}+\frac{\{(L/a)\,\beta_2^{-1/2}+\lambda_2\}\beta_2B_{2m}}{(n/m)^2+\beta_2}\cosh\frac{m\pi\beta_2^{1/2}}{2}\right]. \quad .. \quad (30)$$

The constants A_{1n}, A_{2n}, B_{1m} and B_{2m} may now be determined from the infinite sets of simultaneous equations provided by equations (27), (28), (29) and (30). These equations may be solved numerically by the method of segments and it is then possible to evaluate the distorted shape and stress distribution throughout the entire wing structure.

APPENDIX III

The Flexural Case
Specialisation of Equations for Rigid Ribs

When the ribs may be assumed rigid in their own plane there is a considerable simplification of the analysis and computation. This simplification corresponds to the conventional solution[1], but the equations will be derived here for the sake of completeness.

For equilibrium of an elemental portion of the reinforced skin at $z = b$ (Fig. 2), it is now only necessary for

$$\frac{1}{L}\frac{\partial T}{\partial \xi}+\frac{1}{a}\frac{\partial S}{\partial \eta}=0. \quad .. \quad .. \quad .. \quad .. \quad .. \quad .. \quad .. \quad (31)$$

The stress resultants in terms of the displacements are

$$\left.\begin{aligned} T &= \frac{Et^*}{L}\frac{\partial u}{\partial \xi} \\ S &= \frac{Et}{2(1+\sigma)a}\frac{\partial u}{\partial \eta} \end{aligned}\right\}, \quad .. \quad .. \quad .. \quad .. \quad .. \quad .. \quad .. \quad (32)$$

since the displacement v is zero by virtue of the rigid ribs and symmetry. The equation of equilibrium in terms of the displacement u is then found to be

$$\beta\frac{\partial^2 u}{\partial \xi^2}+\frac{\partial^2 u}{\partial \eta^2}=0, \quad .. \quad .. \quad .. \quad .. \quad .. \quad .. \quad .. \quad .. \quad .. \quad (33)$$

(or (4) bis)

where β is a non-dimensional structural constant such that

$$\beta=\left(\frac{a}{L}\right)^2 2(1+\sigma)\left(\frac{t^*}{t}\right).$$

This equation has the solution

$$u = \frac{1}{Et} \sum_{n=1}^{\infty} A_n \sin \frac{n\pi\xi}{2} \cosh \frac{n\pi\beta^{1/2}\eta}{2} , \quad \ldots \quad (34) \text{ (or (5) bis)}$$

where n is an odd integer and the A_n are constants to be determined. From equations (15) and (16) it is found for compatibility of strain between the rear spar boom and the adjacent reinforced skin it is necessary that

$$\frac{\partial u}{\partial \xi}\Big/_{\eta=1} = - \frac{L^2}{EA} \int_{\xi}^{1} (S_R + S/_{\eta=1})\, d\xi \, .$$

Substituting equations (22), (32) and (34) into this last, the coefficients A_n are found to be

$$A_n = \frac{(2LZ_R)2\left(\dfrac{L}{b}\right)\left[1 - \dfrac{(-)^{(n-1)/2}2}{n\pi}\right]}{n^2\pi^2\left\{\left(\dfrac{t^*}{t}\right)\left(\dfrac{a}{L}\right)\beta^{-1/2} \sinh \dfrac{n\pi\beta^{1/2}}{2} + \dfrac{1}{2}\left(\dfrac{A}{Lt}\right) n\pi \cosh \dfrac{n\pi\beta^{1/2}}{2}\right\}} \quad \ldots \quad (35)$$

where $Z_R(\xi)$ has been assumed constant along each spar.

The z-wise displacement is given by equation (20), *viz.*,

$$w_R = \bar{w} = \frac{2(1+\sigma)}{Et_R} L \int_0^{\xi} S_R \, d\xi - \frac{L}{b} \int_0^{\xi} u/_{\eta=1} d\xi \, , \quad \ldots \quad (36)$$

there being no variation of $\bar{w}$ along a chord because the ribs are rigid.

APPENDIX IV

The Flexural Case

Convergence of the Series Solutions at the Spar Booms

Before proceeding with a numerical calculation it is advisable to examine the convergence of the series solution. For example, when the ribs are considered rigid and the loading is uniform along the spar booms, the direct stress along the stringers is given by

$$\frac{E}{L}\frac{\partial u}{\partial \xi} = \frac{(2LZ_R)}{bt} \sum_{n=1}^{\infty} \frac{\left[1 - \dfrac{(-)^{(n-1)/2}\,2}{n\pi}\right] \cos \dfrac{n\pi\xi}{2} \cosh \dfrac{n\pi\beta^{1/2}\eta}{2}}{n\pi \left\{\left(\dfrac{t^*}{t}\right)\left(\dfrac{a}{L}\right)\beta^{-1/2} \sinh \dfrac{n\pi\beta^{1/2}}{2} + \dfrac{1}{2}\left(\dfrac{A}{Lt}\right) n\pi \cosh \dfrac{n\pi\beta^{1/2}}{2}\right\}} \quad (37)$$

from equations (32), (34) and (35). Now, at $\xi = 0$, $\eta = 1$ this series for the stress converges as $1/n^2$ which is unsatisfactory from the numerical calculation standpoint. However, for equilibrium across a chordwise section it is necessary that

$$Et^*\left(\frac{a}{L}\right)\int_{-1}^{1} \frac{\partial u}{\partial \xi} d\eta + 2\frac{EA}{L}\frac{\partial u}{\partial \xi}\Big/_{\eta=1} = \frac{L}{b}\int_{\xi}^{1} (\xi' - \xi)\, Z_R(\xi')\, d\xi'$$

and so stress along the rear spar boom, *i.e.*, at $\eta = 1$, is now given by

$$\frac{E}{L}\frac{\partial u}{\partial \xi}\Big/_{\eta=1} = \frac{L}{2Ab}\int_{\xi}^{1} (\xi' - \xi)\, Z_R(\xi')\, d\xi' - \frac{Et^*}{2A}\left(\frac{a}{L}\right)\int_{-1}^{1} \frac{\partial u}{\partial \xi} d\eta \, . \quad \ldots \quad (38)$$

B

Substituting equation (37) into this last and assuming $Z_R(\xi)$ to be constant along the spars, it is found that

$$EL \frac{\partial u}{\partial \xi} \Big/_{\eta=1} = (2LZ_R) \frac{L(1-\xi)^2}{8Ab}$$

$$- (2LZ_R) \frac{2at^*}{bAt\beta^{1/2}} \sum_{n=1}^{\infty} \frac{\left[1 - \frac{(-)^{(n-1)/2}\,2}{n\pi}\right] \cos \frac{n\pi\xi}{2} \sinh \frac{n\pi\beta^{1/2}}{2}}{n^2\pi^2 \left\{\left(\frac{t^*}{t}\right)\left(\frac{a}{L}\right)\beta^{-1/2} \sinh \frac{n\pi\beta^{1/2}}{2} + \frac{1}{2}\left(\frac{A}{Lt}\right) n\pi \cosh \frac{n\pi\beta^{1/2}}{2}\right\}} \quad \ldots \quad (39)$$

so the series for the stress along the rear spar boom now converges as $1/n^3$.

It is difficult to examine analytically the convergence of the solution in Appendix II, but it is to be expected that the series will behave similarly to the above. Proceeding in a similar manner, it is necessary for equilibrium across a chordwise section for

$$\frac{Et}{1-\sigma^2} \int_{-1}^{1} \left\{\alpha^* \left(\frac{a}{L}\right) \frac{\partial u}{\partial \xi} + \sigma \frac{\partial v}{\partial \eta}\right\} d\eta + \frac{2EA}{L} \frac{\partial u}{\partial \xi} \Big/_{\eta=1}$$

$$= \frac{aL}{2b} \int_{\xi}^{1} \int_{-1}^{1} (\xi' - \xi)\, Z(\xi', \eta)\, d\eta\, d\xi' + \frac{L}{b} \int_{\xi}^{1} (\xi' - \xi)\, Z_R(\xi')\, d\xi'$$

and so the stress along the rear spar boom is now given by

$$\frac{E}{L} \frac{\partial u}{\partial \xi} \Big/_{\eta=1} = \frac{aL}{4Ab} \int_{\xi}^{1} \int_{-1}^{1} (\xi' - \xi)\, Z(\xi', \eta)\, d\eta\, d\xi' + \frac{L}{2Ab} \int_{\xi}^{L} (\xi' - \xi) Z_R(\xi')\, d\xi'$$

$$- \frac{Et}{2A(1-\sigma^2)} \int_{-1}^{1} \left\{\alpha^* \left(\frac{a}{L}\right) \frac{\partial u}{\partial \xi} + \sigma \frac{\partial v}{\partial \eta}\right\} d\eta \,. \quad \ldots \quad \ldots \quad \ldots \quad (40)$$

Substituting equations (23) and (25) into this last and integrating yields

$$\frac{E}{L} \frac{\partial u}{\partial \xi} \Big/_{\eta=1} = (2aLZ + 2LZ_R) \frac{L(1-\xi)^2}{8Ab} + (2aLZ) \frac{\sigma a^2}{12AbL\bar{a}}$$

$$- \frac{1}{A} \sum_{n=1}^{\infty} \cos \frac{n\pi\xi}{2} \left[\left\{\left(\frac{a}{L}\right) \alpha^* \beta_1^{1/2} - \sigma\lambda_1\right\} A_{1n} \sinh \frac{n\pi\beta_1^{-1/2}}{2}\right.$$

$$\left. + \left\{\left(\frac{a}{L}\right) \alpha^* \beta_2^{1/2} - \sigma\lambda_2\right\} A_{2n} \sinh \frac{n\pi\beta_2^{-1/2}}{2}\right]$$

$$- \frac{1}{A} \sum_{m=1}^{\infty} (-)^{(m-1)/2} \left[\left\{\left(\frac{a}{L}\right) \alpha^* \beta_1^{1/2} - \sigma\lambda_1\right\} B_{1m} \cosh \frac{m\pi\beta_1^{1/2}\xi}{2}\right.$$

$$\left. + \left\{\left(\frac{a}{L}\right) \alpha^* \beta_2^{1/2} - \sigma\lambda_2\right\} B_{2m} \cosh \frac{m\pi\beta_2^{1/2}\xi}{2}\right]. \quad \ldots \quad \ldots \quad \ldots \quad (41)$$

so that the convergence of the series for the stress along the rear spar has been improved by $1/n$, The order of convergence for the stress in the rib booms at $\eta = 1$ is the same as for the stress along the spar booms. However, the rib boom stress at $\eta = 1$ can be calculated from the boundary condition $T' = 0$ along $\eta = 1$, i.e.,

$$\frac{E}{a}\frac{\partial v}{\partial \eta}\bigg/_{\eta=1} = -\frac{E}{L}\frac{\sigma}{\alpha^*}\frac{\partial u}{\partial \xi}\bigg/_{\eta=1} \quad \ldots \quad (42)$$

and using the value of $\frac{E}{L}\frac{\partial u}{\partial \xi}\bigg/_{\eta=1}$ obtained from equation (41).

The convergence of the series for the shear stress in the reinforced skins along the spar booms is not satisfactory and it is not possible to improve the convergence in a similar manner to the above. However, the shear stresses in the reinforced skins are small and therefore are not of such great importance.

APPENDIX V

The Flexural Case
Numerical Illustrative Example

1. *General.*—The numerical illustrative example is based on a wing whose structural box has an aspect ratio 2 and thickness/chord ratio 7·5 per cent. The values of the structural constants are :

a	=	100 in.	Semi-chord dimension
A	=	10 in.^{2}	Cross-sectional area of the front and rear spar booms
b	=	7·5 in.	Semi-spar depth
L	=	200 in.	Semi-span dimension
t	=	0·15 in.	Nominal thickness of top and bottom skins
t_R	=	0·15 in.	Nominal thickness of the front and rear spar webs
t^*	=	0·20 in.	Effective thickness of the skin-stringer combination for resisting load in the direction of the stringers
$\bar{t}$	=	0·18 in.	Effective thickness of the skin–rib-boom combination for resisting load in the direction of the ribs
τ	=	0·008	Thickness of rib webs per unit length of span
E	=	10^7 lb/in.^{2}	Young's modulus of elasticity for the structure
σ	=	0·3	Poisson's ratio for the structure.

2. *Numerical Example for Appendix II.*—The above give the following values of the non-dimensional structural parameters for the exact solution :

$\alpha^* = 1 \cdot 303333$

$\bar{\alpha} = 1 \cdot 182000$

$\beta_1 = 1 \cdot 556712$

$\beta_2 = 9 \cdot 321242$

$\lambda_1 = 0 \cdot 3877429$

$\lambda_2 = 2 \cdot 708165.$

For the purpose of these calculations the particular loading cases of

$$2aLZ(\xi,\eta) = 2aLZ = 1\cdot 0 \text{ lb.}$$

$$2LZ_R(\xi) = 2LZ_R = 1\cdot 0 \text{ lb}$$

have been chosen.

The values of the constants A_{1n}, A_{2n}, B_{1m}, B_{2m} are determined from equations (27) to (30) by the method of segments, *i.e.*, it is assumed that $A_{1n} = A_{2n} = B_{1m} = B_{2m} = 0$, when $n, m > 9$ say. This then yields twenty simultaneous equations for the determination of twenty constants. The general scheme of these equations is depicted below,

A_{11}	A_{13}	A_{15}	A_{17}	A_{19}	B_{11}	B_{13}	B_{15}	B_{17}	B_{19}	A_{21}	A_{23}	A_{25}	A_{27}	A_{29}	B_{21}	B_{23}	B_{25}	B_{27}	B_{29}	= constant
X										X										= 0
	X										X									= 0
		X										X								= 0
			X										X							= 0
				X										X						= 0
					X										X					= X
						X										X				= X
							X										X			= X
								X										X		= X
									X										X	= X
X	X	X	X	X	X					X	X	X	X	X	X					= 0
X	X	X	X	X		X				X	X	X	X	X		X				= 0
X	X	X	X	X			X			X	X	X	X	X			X			= 0
X	X	X	X	X				X		X	X	X	X	X				X		= 0
X	X	X	X	X					X	X	X	X	X	X					X	= 0
X					X	X	X	X	X	X					X	X	X	X	X	= X
	X				X	X	X	X	X		X				X	X	X	X	X	= X
		X			X	X	X	X	X			X			X	X	X	X	X	= X
			X		X	X	X	X	X				X		X	X	X	X	X	= X
				X	X	X	X	X	X					X	X	X	X	X	X	= X

and they readily reduce to a set of five simultaneous equations where the leading diagonal terms are predominant. These equations were then rapidly solved by an iterative method and yielded the following values for the constants :

$A_{11} = 1\cdot 40111,$	$A_{21} = -0\cdot 56807,$
$A_{13} = 0\cdot 20252 \times 10^{-1},$	$A_{23} = -0\cdot 43741 \times 10^{-1},$
$A_{15} = 0\cdot 34523 \times 10^{-3},$	$A_{25} = -0\cdot 34341 \times 10^{-2},$
$A_{17} = 0\cdot 11321 \times 10^{-4},$	$A_{27} = -0\cdot 50168 \times 10^{-3},$
$A_{19} = 0\cdot 43504 \times 10^{-6},$	$A_{29} = -0\cdot 85506 \times 10^{-4},$
$B_{11} = -0\cdot 61064 \times 10^{-1},$	$B_{21} = 0\cdot 41136 \times 10^{-2},$
$B_{13} = 0\cdot 51276 \times 10^{-4},$	$B_{23} = -0\cdot 77737 \times 10^{-8},$
$B_{15} = -0\cdot 12043 \times 10^{-6},$	$B_{25} = 0\cdot 64103 \times 10^{-13},$
$B_{17} = 0\cdot 84497 \times 10^{-9},$	$B_{27} = -0\cdot 14552 \times 10^{-17},$
$B_{19} = -0\cdot 91497 \times 10^{-11},$	$B_{29} = 0\cdot 51053 \times 10^{-22}$

for the loading case $2aLZ = 1 \cdot 0$, and

$$\begin{aligned}
A_{11} &= 1 \cdot 34792, & A_{21} &= -0 \cdot 54649, \\
A_{13} &= 0 \cdot 20195 \times 10^{-1}, & A_{23} &= -0 \cdot 43618 \times 10^{-1}, \\
A_{15} &= 0 \cdot 34800 \times 10^{-3}, & A_{25} &= -0 \cdot 34616 \times 10^{-2}, \\
A_{17} &= 0 \cdot 11236 \times 10^{-4}, & A_{27} &= -0 \cdot 49791 \times 10^{-3}, \\
A_{19} &= 0 \cdot 43799 \times 10^{-6}, & A_{29} &= -0 \cdot 86086 \times 10^{-4}, \\
B_{11} &= -0 \cdot 14491, & B_{21} &= 0 \cdot 51316 \times 10^{-2}, \\
B_{13} &= 0 \cdot 66823 \times 10^{-4}, & B_{23} &= -0 \cdot 79862 \times 10^{-8}, \\
B_{15} &= -0 \cdot 15034 \times 10^{-6}, & B_{25} &= 0 \cdot 61839 \times 10^{-13}, \\
B_{17} &= 0 \cdot 95873 \times 10^{-9}, & B_{27} &= -0 \cdot 13572 \times 10^{-17}, \\
B_{19} &= -0 \cdot 97057 \times 10^{-11}, & B_{29} &= 0 \cdot 47288 \times 10^{-22},
\end{aligned}$$

for the loading case $2LZ_R = 1 \cdot 0$. Substituting these values into the equations of Appendices I and II it is possible to obtain the distorted shape and the stress distribution for the wing structure. The stress distributions are shown in Figs. 6 to 15 where the values of $\left.\frac{E}{L}\frac{\partial u}{\partial \xi}\right/_{\eta=1}$ and $\left.\frac{E}{a}\frac{\partial v}{\partial \eta}\right/_{\eta=1}$ were obtained by the method of Appendix IV. The distorted shape of the wing structure is shown in Figs. 16 and 17.

It now only remains to show that a sufficient number of terms have been taken for satisfactory convergence of the spar boom stress at the root. The above calculations were therefore repeated for $A_{1n} = A_{2n} = B_{1m} = B_{2m} = 0$, when $n, m > 7$ and the results are compared with the more accurate calculation in the table below :—

	Uniformly distributed load over whole surface, $2aLZ = 1 \cdot 0$ lb	Uniformly distributed load along the spars, $2LZ_R = 1 \cdot 0$ lb
Max. spar-boom stress (*i.e.*, at $\xi = 0, \eta = 1$) $n, m = 1, 3, 5, 7$	$0 \cdot 2043$ lb/in.^{2}	$0 \cdot 2006$ lb/in.^{2}
Max. spar-boom stress (*i.e.*, at $\xi = 0, \xi = 1$) $n, m = 1, 3, 5, 7, 9$	$0 \cdot 2036$ lb/in.^{2}	$0 \cdot 1999$ lb/in.^{2}

From the above table it appears satisfactory to terminate the series after $n, m = 1, 3, 5, 7, 9$.

3. *Numerical Example for Appendix III.*—When the ribs may be assumed rigid there is a considerable simplification in the computation. The value of the non-dimensional parameter β is found to be $\beta = 0 \cdot 866667$, and the values of the constants A_n when evaluated from equation (35) are found to be :

$$\begin{aligned}
A_1 &= 0 \cdot 74016 \\
A_3 &= 0 \cdot 7917 \times 10^{-2} \\
A_5 &= 0 \cdot 7555 \times 10^{-4} \\
A_7 &= 0 \cdot 1969 \times 10^{-5} \\
A_9 &= 0 \cdot 4395 \times 10^{-7} .
\end{aligned}$$

Using these values the stress distribution and distorted shape have been calculated and are compared with the exact results in Figs. 6 to 17.

The spar-boom stress at the root, calculated from the method of Appendix IV, is 0·1955 lb/in.² using the above values, and is 0·1963 lb/in.² using only the terms for $n = 1, 3, 5, 7$. Hence it appears satisfactory to terminate the series after $n = 1, 3, 5, 7, 9$†.

APPENDIX VI

The Flexural Case

Simplified Method for the Determination of the Additional Effects Due to the Chordwise Distribution of Loading

The additional effects due to the chordwise distribution of loading, *i.e.*, due to the statically zero loading $2aLZ - 2LZ_R$, can be approximately assessed by assuming that the wing span is infinite.

When $2aLZ = 2LZ_R = 1 \cdot 0$ lb, the surface force $\bar{S}$ is found from equation (17) to be

$$\bar{S} = \frac{\eta}{4bL} \text{ lb/in.}^2 \qquad (43)$$

which is self-equilibriating. When the wing span is infinite, the solution to equation (13) becomes

$$\left.\begin{aligned} u &= \frac{1-\sigma^2}{Et}\left(\frac{L}{a}\right)\xi C_1 \\ v &= \frac{1-\sigma^2}{Et}\,\frac{1}{8}\left(\frac{a^2}{bL}\right)\frac{1}{\bar{a}}\left(\frac{\eta^3}{3} + \eta C_2\right) \end{aligned}\right\} \qquad (44)$$

where C_1 and C_2 are constants to be determined from the boundary conditions. The stress resultants in the reinforced skins are found to be

$$\left.\begin{aligned} T &= \frac{\alpha^*}{a} C_1 + \frac{1}{8}\left(\frac{a^2}{bL}\right)\frac{\sigma}{a\bar{a}}(\eta^2 + C_2) \\ T' &= \frac{1}{8}\left(\frac{a^2}{bL}\right)\frac{1}{a}(\eta^2 + C_2) + \frac{\sigma}{a} C_1 \\ S &= 0 \end{aligned}\right\} \qquad (45)$$

from equation (12). Now, the boundary conditions are

$$\left.\begin{aligned} &T' = 0 \text{ at } \eta = 1 \\ &a\int_{-1}^{1} T\,d\eta + \frac{2EA}{L}\frac{\partial u}{\partial \xi}\bigg/_{\eta=1} = 0 \end{aligned}\right\} \qquad (46)$$

Substitution of equations (45) into these last yield the following values for the constants

$$\left.\begin{aligned} C_1 &= \left(\frac{a^2}{bL}\right) 12\bar{a}\left(\frac{A}{at}\frac{1-\sigma^2}{\sigma} + \frac{\alpha^*}{\sigma} - \frac{\sigma}{\bar{a}}\right) \\ C_2 &= -1 - 2\sigma/3\bar{a}\left(\frac{A}{at}\frac{1-\sigma^2}{\sigma} + \frac{\alpha^*}{\sigma} - \frac{\sigma}{\bar{a}}\right) \end{aligned}\right\} \qquad (47)$$

---

† If the series is terminated after $n = 1, 3, 5, 7, 9, 11, 13, 15, 17, 19$, the spar-boom stress at the root is 0·1942 lb/in.².

Substitution of the values of the structural constants used in Appendix V for the numerical example yields

$$C_1 = 0\cdot0007689$$

$$C_2 = -\ 1\cdot0277.$$

Using these values and the results of Appendix V it is found that :

	Statically zero distributed load $2aLZ - 2LZ_R$ acting on a wing of infinite span	Statically zero distributed load $2aLZ - 2LZ_R$ acting on the wing investigated in Appendix V
Spar-boom stress at $\xi = 0,\ \eta = 1$	$0\cdot0047$ lb/in.^{2}	$0\cdot0037$ lb/in.^{2}
Rib-boom stress at $\xi = 0,\ \eta = 0$	$-0\cdot0440$ lb/in.^{2}	$-0\cdot0453$ lb/in.^{2}
Rib-boom stress at $\xi = 1,\ \eta = 0$	$-0\cdot0440$ lb/in.^{2}	$-0\cdot0380$ lb/in.^{2}
z-wise deflection at centre of tip rib	$-0\cdot273 \times 10^{-5}$ in.	$-0\cdot313 \times 10^{-5}$ in.
z-wise deflection at centre of root rib	$-0\cdot273 \times 10^{-5}$ in.	$-0\cdot279 \times 10^{-5}$ in.

From the above table it is seen that the additional effects due to the chordwise distribution of loading on a wing may be approximately assessed by the simplified method developed in this Appendix.

APPENDIX VII

The Flexural Case

Anti-clastic Effects in Pure Bending

In considering the chordwise distortion of the wing it is of interest to compare the actual distortion with the anti-clastic effect produced by pure bending.

If the bending moment is M, then the stress resultants in the reinforced skin are

$$\left.\begin{aligned} T &= \frac{Mt^*}{2b(A + at^*)} \\ T' &= 0 \\ S &= 0 \end{aligned}\right\} \quad \ldots \qquad (48)$$

Now, from equation (12) it is seen for T' to be zero it is necessary that

$$\frac{1}{a}\frac{\partial v}{\partial \eta} = -\frac{\sigma}{\bar{a}}\frac{1}{L}\frac{\partial u}{\partial \xi}$$

whence

$$\frac{1}{a}\frac{\partial v}{\partial \eta} = -\ T\,\frac{1-\sigma^2}{Et\left(\alpha^* - \dfrac{\sigma^2}{\bar{a}}\right)}\,\frac{\sigma}{\bar{a}},$$

and, on integrating,

$$v = - T \frac{1 - \sigma^2}{Et\left(\alpha^* - \dfrac{\sigma^2}{\bar{a}}\right)} \frac{\sigma}{\bar{a}} a\eta \; . \quad .. \quad .. \quad .. \quad .. \quad .. \quad .. \qquad (49)$$

The chordwise distortion is given by

$$\bar{w} = \frac{a}{b} \int_{\eta}^{1} v \, d\eta$$

from equation (21), and substituting equation (49) into this last it is found that

$$\bar{w} = - T \frac{1 - \sigma^2}{Et\left(\alpha^* - \dfrac{\sigma^2}{\bar{a}}\right)} \frac{\sigma}{\bar{a}} \frac{a^2}{2b} (1 - \eta^2) \; . \quad .. \quad .. \quad .. \quad .. \quad .. \qquad (50)$$

Substitution of the values of the structural constants used in Appendix V for the numerical example yields an anti-clastic deflection of $- 0 \cdot 186 \times 10^{-5}$ in. for a tip moment of $L^2 Z_R = L/2$ in. lb.

APPENDIX VIII

The Torsional Case
Derivation of Fundamental Equations Using a Variational Procedure

The torsional case corresponds to a loading anti-symmetrically distributed about the spanwise centre-line of the wing box. Unlike the flexural case, the spar and rib web shears are no longer statically determinate and so the problem is three-dimensional. The analysis could, however, proceed in a similar manner as Appendix I but the algebra and computation would be correspondingly more intricate and so a rather different approach has been favoured. In what follows, attention is confined to cases where the displacements u, v at $z = \pm b$ are equal and opposite to one another.

1. *Fundamental Equations.*—For equilibrium of an elemental portion of the reinforced skin at $z = b$ (Fig. 2), it is necessary that

$$\left.\begin{aligned} \left(\frac{a}{L}\right) \frac{\partial T}{\partial \xi} + \frac{\partial S}{\partial \eta} &= 0 \\ \left(\frac{a}{L}\right) \frac{\partial S}{\partial \xi} + \frac{\partial T'}{\partial \eta} - a\bar{S} &= 0 \\ \bar{S} &= \frac{1}{L} \frac{d}{d\xi} \int_0^1 S \, d\eta \end{aligned}\right\} , \quad .. \quad .. \quad .. \quad .. \quad .. \quad .. \qquad \begin{array}{r}(51) \\ \text{or (6) bis}\end{array}$$

where the last equation is obtained from consideration of the equilibrium of a strip $L\delta\xi$ across the chord of the box and where it is assumed that there is no distributed load along the chord (equation (17)).

A consistent system of stress resultants satisfying equation (51) is then

$$\left.\begin{aligned}
T &= \sum_{n=1}^{\infty} \eta^n F_n(\xi) \\
T' &= -\left(\frac{a}{L}\right)^2 \frac{d^2}{d\xi^2} \sum_{n=1}^{\infty} \frac{\eta(1-\eta^{n+1})}{(n+1)(n+2)} F_n(\xi) \\
S &= -\left(\frac{a}{L}\right) \frac{d}{d\xi} \left\{F(\xi) + \sum_{n=1}^{\infty} \frac{\eta^{n+1}}{n+1} F_n(\xi)\right\} \\
\bar{S} &= -\frac{1}{L}\left(\frac{a}{L}\right) \frac{d^2}{d\xi^2} \left\{F(\xi) + \sum_{n=1}^{\infty} \frac{1}{(n+1)(n+2)} F_n(\xi)\right\}
\end{aligned}\right\} , \quad \ldots \quad \ldots \quad \begin{array}{r}(52)\\ \text{or (7) bis.}\end{array}$$

where n is an odd integer and $F(\xi)$, $F_n(\xi)$ are functions to be determined from the condition that the strain energy is made a minimum.

Since the effect of the chordwise distribution of loading will, in general, be smaller than for the flexural case, it will be assumed that there is only an equal and opposite distribution of loading along the two spars. In particular, it is assumed for the remainder of this analysis that this loading is uniform, *i.e.*,

$$Z_R(\xi) = Z_R = \text{a constant} . \quad \ldots \quad \ldots \quad \ldots \quad \ldots \quad \ldots \quad \ldots \quad \ldots \quad (53)$$

For this loading, the equation of overall equilibrium is

$$S_R = \int_0^1 S\, d\eta - \frac{(2LZ_R)}{4b}(1-\xi) \quad \ldots \quad \ldots \quad \ldots \quad \ldots \quad \ldots \quad \ldots \quad (54)$$

obtained from resolution of the torque at a chordwise section. Substituting equations (52) into this last, the spar-web shear-stress resultant is found to be

$$S_R = -\frac{(2LZ_R)}{4b}(1-\xi) - \frac{a}{L}\frac{d}{d\xi}\left\{F(\xi) + \sum_{n=1}^{\infty} \frac{1}{(n+1)(n+2)} F_n(\xi)\right\} . \quad (55)$$

Finally, substitution of equations (52) and (55) into equation (14) yields the spar-boom load :

$$P_R = (2LZ_R)\frac{1}{8}\left(\frac{L}{b}\right)(1-\xi)^2 - a\left\{2F(\xi) + \sum_{n=1}^{\infty} \frac{n+3}{(n+1)(n+2)} F_n(\xi)\right. \quad \ldots \quad (56)$$

provided that $F(1)$ and $F_n(1)$ are all zero, and the stress distribution throughout the whole wing box has now been defined in terms of the unknown functions $F(\xi)$ and $F_n(\xi)$.

The total strain energy stored in the wing box is, apart from an irrelevant factor :

$$S.E. = \left(\frac{a}{t}\right)\int_0^1\int_0^1\left\{\frac{1-\sigma^2}{\alpha^*\bar{a}-\sigma^2}\left(\bar{a}T^2-2\sigma TT'+\alpha^*T'^2\right)+2(1+\sigma)S^2\right\}d\xi\, d\eta$$

$$+\int_0^1\left\{2(1+\sigma)\left(\frac{b}{t_R}\right)S_R^{\,2}+\frac{P_R^{\,2}}{A}+2(1+\sigma)\frac{ab}{\tau}\bar{S}^2\right\}d\xi\,. \qquad \text{(57)}$$

For the strain energy to be a minimum, each arbitrary variation δF or δF_m must be made zero so that

$$\left(\frac{a}{t}\right)\int_0^1\int_0^1\left[\frac{1-\sigma^2}{\alpha^*\bar{a}-\sigma^2}\left\{(\bar{a}T-\sigma T')\frac{dT}{dF_m}\delta F_m+(\alpha^*T'-\sigma T)\frac{dT'}{dF_m''}\delta F_m''\right\}\right.$$

$$\left.+\,2(1+\sigma)S\frac{dS}{dF_m'}\delta F_m'\right]d\xi\, d\eta$$

$$+\int_0^1\left\{2(1+\sigma)\left(\frac{b}{t_R}\right)S_R\frac{dS_R}{dF'_m}\delta F_m'+\frac{P_R}{A}\frac{dP_R}{dF_m}\delta F_m+2(1+\sigma)\frac{ab}{\tau}\bar{S}\frac{d\bar{S}}{dF_m''}\delta F_m''\right\}d\xi=0\,,$$

where F_m', F_m'' denote differentiations with respect to ξ. Using the usual arguments of the Calculus of Variations it is found that

$$\left(\frac{a}{t}\right)\int_0^1\left[\frac{1-\sigma^2}{\alpha^*\bar{a}-\sigma^2}\left\{(\bar{a}T-\sigma T')\frac{dT}{dF_m}+\frac{d^2}{d\xi^2}(\alpha^*T'-\sigma T)\frac{dT'}{dF_m''}\right\}-2(1+\sigma)\frac{dS}{d\xi}\frac{dS}{dF_m'}\right]d\eta$$

$$-\,2(1+\sigma)\left(\frac{b}{t_R}\right)\frac{dS_R}{d\xi}\frac{dS_R}{dF_m'}+\frac{P_R}{A}\frac{dP_R}{dF_m}+2(1+\sigma)\frac{ab}{\tau}\frac{d^2\bar{S}}{d\xi^2}\frac{d\bar{S}}{dF_m''}=0, \qquad \text{(58)}$$

with the boundary conditions

$$\left[\left(\frac{a}{t}\right)\int_0^1\left\{-\frac{1-\sigma^2}{\alpha^*\bar{a}-\sigma^2}\frac{d}{d\xi}(\alpha^*T'-\sigma T)\frac{dT'}{dF_m''}+2(1+\sigma)S\frac{dS}{dF_m'}\right\}\delta F_m\, d\eta\right.$$

$$\left.+\,2(1+\sigma)\left(\frac{b}{t_R}\right)S_R\frac{dS_R}{dF_m'}\delta F_m-2(1+\sigma)\frac{ab}{\tau}\frac{d\bar{S}}{d\xi}\frac{d\bar{S}}{dF_m''}\delta F_m\right]_0^1, \qquad \text{(59)}$$

and

$$\left[\left(\frac{a}{t}\right)\int_0^1\frac{1-\sigma^2}{\alpha^*\bar{a}-\sigma^2}(\alpha^*T'-\sigma T)\frac{dT'}{dF_m''}\delta F_m'\, d\eta+2\,(1+\sigma)\frac{ab}{\tau}\bar{S}\frac{d\bar{S}}{dF_m''}\delta F_m'\right]_0^1. \qquad \text{(60)}$$

It is more convenient to express the first boundary condition, equation (59), in the form

$$\left[\left(\frac{a}{t}\right)\int\int_0^1\frac{1-\sigma^2}{\alpha^*\bar{a}-\sigma^2}(\bar{a}T-\sigma T')\frac{dT}{dF_m}\delta F_m\, d\eta\, d\xi+\frac{1}{A}\int P_R\frac{dP_R}{dF_m}\delta F_m\, d\xi\right]_0^1=0, \qquad \text{(61)}$$

where the constants of integration are determined from equation (59).

Substituting equations (52) into equation (58), the differential equations in terms of F and F_n are found to be

$$\left.\begin{aligned}
&2(1+\sigma)\left(\frac{a^3b}{L^4}\right)\frac{1}{\tau}\left\{\frac{d^4F}{d\xi^4}+\sum_{n=1}^{\infty}\frac{1}{(n+1)(n+2)}\frac{d^4F_n}{d\xi^4}\right\}\\
&\quad-2(1+\sigma)\left(\frac{a}{t}+\frac{b}{t_R}\right)\left(\frac{a}{L}\right)^2\left\{\frac{d^2F}{d\xi^2}+\sum_{n=1}^{\infty}\frac{1}{(n+1)(n+2)}\frac{d^2F_n}{d\xi^2}\right\}\\
&\quad+\frac{2a^2}{A}\left\{2F+\sum_{n=1}^{\infty}\frac{n+3}{(n+1)(n+2)}F_n\right\}\\
&=-2(1+\sigma)\left(\frac{b}{t_R}\right)\left(\frac{a}{L}\right)\frac{(2LZ_R)}{4b}+\frac{(2LZ_R)}{4b}\left(\frac{aL}{A}\right)(1-\xi)^2,\\
&\text{and the } m\text{th equation}\\
&2(1+\sigma)\left(\frac{a^3b}{L^4}\right)\frac{1}{\tau}\frac{1}{(m+1)(m+2)}\left\{\frac{d^4F}{d\xi^4}+\sum_{n=1}^{\infty}\frac{1}{(n+1)(n+2)}\frac{d^4F_n}{d\xi_4}\right\}\\
&\quad+\left(\frac{a}{t}\right)\frac{1-\sigma^2}{\alpha^*\bar{a}-\sigma^2}\alpha^*\left(\frac{a}{L}\right)^4\frac{1}{3(m+2)(m+4)}\sum_{n=1}^{\infty}\frac{n+m+8}{(n+2)(n+4)(n+m+5)}\frac{d^4F_n}{d\xi^4}\\
&\quad-2(1+\sigma)\left(\frac{a}{t}\right)\left(\frac{a}{L}\right)^2\frac{1}{m+1}\left\{\frac{1}{m+2}\frac{d^2F}{d\xi^2}+\sum_{n=1}^{\infty}\frac{1}{(n+1)(n+m+3)}\frac{d^2F_n}{d\xi^2}\right\}\\
&\quad-2(1+\sigma)\left(\frac{b}{t_R}\right)\left(\frac{a}{L}\right)^2\frac{1}{(m+1)(m+2)}\left\{\frac{d^2F}{d\xi^2}+\sum_{n=1}^{\infty}\frac{1}{(n+1)(n+2)}\frac{d^2F_n}{d\xi^2}\right\}\\
&\quad+\left(\frac{a}{t}\right)\frac{1-\sigma^2}{\alpha^*\bar{a}-\sigma^2}2\sigma\left(\frac{a}{L}\right)^2\frac{1}{m+2}\sum_{n=1}^{\infty}\frac{1}{(n+2)(n+m+3)}\frac{d^2F_n}{d\xi^2}\\
&\quad+\frac{a^2}{A}\frac{m+3}{(m+1)(m+2)}\left\{2F+\sum_{n=1}^{\infty}\frac{n+3}{(n+1)(n+2)}F_n\right.\\
&\quad+\left(\frac{a}{t}\right)\frac{1-\sigma^2}{\alpha^*\bar{a}-\sigma^2}\bar{a}\sum_{n=1}^{\infty}\frac{1}{n+m+1}F_n\\
&=-2(1+\sigma)\left(\frac{b}{t_R}\right)\left(\frac{a}{L}\right)\frac{1}{(m+1)(m+2)}\frac{(2LZ_R)}{4b}\\
&\quad+\frac{(2LZ_R)}{8b}\left(\frac{aL}{A}\right)\frac{m+3}{(m+1)(m+2)}(1-\xi)^2
\end{aligned}\right\}. \tag{62}$$

There are thus $(m + 3)/2$ simultaneous differential equations of fourth order involving only the even differentials. The arbitrary constants contained in the complementary functions are determined from the boundary conditions given in equations (60) and (61), *viz.*,

$$\left.\begin{aligned} &\frac{dF}{d\xi} = \frac{dF_m}{d\xi} = 0 \quad \text{at} \quad \xi = 0 \text{ and } \xi = 1 \\ &F = F_m = 0 \text{ at } \xi = 1 \\ &\left(\frac{a}{t}\right)\int\int_0^1 \frac{1-\sigma^2}{\alpha^*\bar{\alpha}-\sigma^2}(\bar{\alpha}T - \sigma T')\frac{dT}{dF_m}\,d\eta\,d\xi + \frac{1}{A}\int P_R\frac{dP_R}{dF_m}\,d\xi = 0 \text{ at } \xi = 0 \end{aligned}\right\} \quad \ldots \quad (63)$$

where the constant of integration for this last equation is determined from equation (59). If the complementary functions are expressed in terms of sinh, cosh, sin and cos functions, equations (63) then yield two sets of $m + 3$ simultaneous equations.

When the functions F, F_n have been determined, the stress distribution throughout the wing can be evaluated by substitution into equations (52), (55) and (56).

The z-wise displacements of the wing are determined from

$$\bar{w} = \frac{2(1+\sigma)}{E\tau}\,a\int_0^\eta \bar{S}\,d\eta - \frac{a}{b}\int_0^\eta v\,d\eta\,, \quad \ldots \quad (64) \text{ or (8) bis}$$

(*cf.* equation (18)), where the displacement v is determined from the stress-strain relationships given in equation (12). The z-wise displacement w_R of the spar booms is given by equation (20) where, of course

$$w_R = \bar{w}/_{\eta=1}. \quad \ldots \quad (65)$$

2. *The Conventional Solution.*—The conventional solution[2] is derived from the aforegoing by putting all the F_n equal to zero. Equations (52) for the stress resultants in the reinforced skins then become

$$\left.\begin{aligned} &T = T' = 0 \\ &S = -\left(\frac{a}{L}\right)\frac{dF}{d\xi} \\ &\bar{S} = -\frac{1}{L}\left(\frac{a}{L}\right)\frac{d^2F}{d\xi^2} \end{aligned}\right\}, \quad \ldots \quad (66)$$

and the differential equation for F is

$$2(1+\sigma)\frac{a^3b}{L^4}\frac{1}{\tau}\frac{d^4F}{d\xi^4} - 2(1+\sigma)\left(\frac{a}{t}+\frac{b}{t_R}\right)\left(\frac{a}{L}\right)^2\frac{d^2F}{d\xi^2} + \frac{4a^2}{A_e}F$$

$$= -2(1+\sigma)\left(\frac{b}{t_R}\right)\left(\frac{a}{L}\right)\frac{(2LZ_R)}{4b} + \frac{(2LZ_R)}{4b}\left(\frac{aL}{A_e}\right)(1-\xi)^2\,, \quad \ldots \quad (67)$$

where A_e is the effective area of the spar booms and is usually taken to be

$$A_e = A + \frac{at^*}{3}. \quad \ldots \quad (68)$$

3. *The Conventional Solution where the Ribs are Assumed Rigid.*—When the ribs are assumed rigid the thickness of ribs τ per unit run becomes infinite and the differential equation for F is then

$$- 2(1 + \sigma)\left(\frac{a}{t} + \frac{b}{t_R}\right)\left(\frac{a}{L}\right)^2 \frac{d^2F}{d\xi^2} + \frac{4a^2}{A_e} F = - 2(1 + \sigma)\left(\frac{b}{t_R}\right)\left(\frac{a}{L}\right) \frac{(2LZ_R)}{4b}$$

$$+ \frac{(2LZ_R)}{4b}\left(\frac{aL}{A_e}\right)(1 - \xi)^2 . \qquad \qquad (69)$$

APPENDIX IX

The Torsional Case
Derivation of Equations when the Rib Booms may be Considered Inextensional

The determination of the cross-sectional distortion is unlikely to be of such importance as for the flexural case since the distortion will be of a smaller order due to the point of inflexion along the spanwise centre-line. This suggests that a simplified analysis would be suitable whereby the rib booms are considered inextensional (*cf.* Appendix III).

The stress resultants in terms of the displacements are now

$$\left.\begin{aligned} T &= \frac{Et^*}{L} \frac{\partial u}{\partial \xi} \\ S &= \frac{Et}{2(1 + \sigma)}\left(\frac{1}{a}\frac{\partial \eta}{\partial \eta} + \frac{1}{L}\frac{dv}{d\xi}\right) \end{aligned}\right\} , \qquad \qquad (70)$$

where the chordwise displacement v is independent of the η co-ordinate because the rib booms are inextensional. The equation of equilibrium in terms of the displacement u is therefore as given in equation (33) which now has the solution

$$u = \frac{1}{Et} \sum_{n=1}^{\infty} A_n \sin \frac{n\pi\xi}{2} \sinh \frac{n\pi\beta^{1/2}\eta}{2} , \qquad \qquad (71)$$

where n is an odd integer and the A_n are constants to be determined. The displacement v is determined by substituting equations (20) and (64) into (65) giving

$$\frac{2(1 + \sigma)}{E\tau} a \int_0^1 \bar{S}\, d\eta - \frac{a}{b} \int_0^1 v\, d\eta = \frac{2(1 + \sigma)}{Et_R} L \int_0^{\xi} S_R\, d\xi - \frac{L}{b} \int_0^{\xi} u/_{\eta=1}\, d\xi .$$

Substituting equations (70) into the last of equations (51) and into equation (54) and then into the above, it is found that

$$\left(\frac{ab}{L^2}\right)\frac{1}{\tau}\frac{d^3v}{d\xi^3} - \left(\frac{a}{t} + \frac{b}{t_R}\right)\frac{dv}{d\xi} = - \left(\frac{L}{a}\right)\left(\frac{a}{t} - \frac{b}{t_R}\right) u/_{\eta=1} - \left(\frac{b}{L}\right)\frac{1}{\tau}\frac{\partial^2 u}{\partial \xi^2}\Big/_{\eta=1}$$

$$- \frac{2(1 + \sigma)}{Et_R} (2LZ_R) \frac{1}{4}\left(\frac{L}{t}\right) , \qquad \qquad (72)$$

where it is assumed that the loading is constant along the spars. This equation has the solution

$$\frac{dv}{d\xi} = \frac{1}{Et}\left(\frac{L}{a}\right)\left\{C_1 \sinh \gamma^{1/2}\xi + C_2 \cosh \gamma^{1/2}\xi + \sum_{n=1}^{\infty} \nu_n A_n \sin \frac{n\pi\xi}{2} \sinh \frac{n\pi\beta^{1/2}}{2}\right\}$$

$$+ \frac{2(1+\sigma)}{Et_R}\left(\frac{L}{t}\right)(2LZ_R)\frac{(1-\xi)}{4\left(\frac{a}{t}+\frac{b}{t_R}\right)}, \qquad \ldots \qquad \ldots \qquad (73)$$

where C_1 and C_2 are arbitrary constants and

$$\gamma = \left(\frac{L^2}{ab}\right)\tau\left(\frac{a}{t}+\frac{b}{t_R}\right),$$

$$\nu_n = \frac{\left(\frac{a}{t}-\frac{b}{t_R}\right) - \left(\frac{ab}{L^2}\right)\frac{1}{\tau}\left(\frac{n\pi}{2}\right)^2}{\left(\frac{a}{t}+\frac{b}{t_R}\right) + \left(\frac{ab}{L^2}\right)\frac{1}{\tau}\left(\frac{n\pi}{2}\right)^2}.$$

Now, at the root the shear-stress resultant S must be zero, i.e., $dv/d\xi = 0$ at $\xi = 0$, and so

$$C_2 = -2(1+\sigma)(2LZ_R)\left(\frac{a}{t_R}\right)\frac{1}{4\left(\frac{a}{t}+\frac{b}{t_R}\right)}. \qquad \ldots \qquad \ldots \qquad \ldots \qquad \ldots \qquad (74)$$

Furthermore, at the tip

$$\int_0^1 S\, d\eta = 0 \quad \text{at} \quad \xi = 1$$

and substituting equations (70), (71) and (73) into this last yields

$$C_1 = -C_2 \coth \gamma^{1/2} - \operatorname{cosec} \gamma^{1/2} \sum_{n=1}^{\infty} (-)^{(n-1)/2} (\nu_n + 1) A_n \sinh \frac{n\pi\beta^{1/2}}{2}. \qquad \ldots \qquad (75)$$

The A_n are determined from the condition of compatibility between the rear spar boom and the adjacent reinforced skin. From equations (15) and (16) this is found to be

$$\left.\frac{\partial u}{\partial \xi}\right/_{\eta=1} = -\frac{L^2}{EA}\int_\xi^1 (S_R + S/_{\eta=1})\, d\xi .$$

Substituting equations (54), (70), (71) and (73) into this last, it is found that

$$\sum_{n=1}^{\infty} \rho_n A_n \cos \frac{n\pi\xi}{2} \sinh \frac{n\pi\beta^{1/2}}{2} = -2\left(\frac{Lt}{A}\right)\frac{\gamma^{-1/2}}{2(1+\sigma)}\{C_1 (\cosh \gamma^{1/2}$$

$$- \cosh \gamma^{1/2}\xi) + C_2(\sinh \gamma^{1/2} - \sinh \gamma^{1/2}\xi)\}$$

$$+ (2LZ_R)\left(\frac{Lt}{A}\right)\left(\frac{a}{b}\right)\frac{\left(\frac{a}{t}-\frac{b}{t_R}\right)}{8\left(\frac{a}{t}+\frac{b}{t_R}\right)}(1-\xi)^2$$

where $$\rho_n = \frac{1}{2}\left(\frac{a}{L}\right) n\pi + \frac{1}{2(1+\sigma)}\left(\frac{Lt}{A}\right)\left(\frac{2}{n\pi} + \beta^{1/2}\coth\frac{n\pi\beta^{1/2}}{2} + \frac{4\nu_n}{n\pi}\right).$$

Expanding the right hand side of this equation in terms of the cosine series, it is found that

$$\rho_n A_n \sinh\frac{n\pi\beta^{1/2}}{2} = -(-)^{(n-1)/2}\left(\frac{Lt}{A}\right)\frac{1}{2(1+\sigma)}\frac{8\gamma^{1/2}}{n\pi\left\{\left(\frac{n\pi}{2}\right)^2+\gamma\right\}}(C_1\cosh\gamma^{1/2} + C_2\sinh\gamma^{1/2})$$

$$+\left(\frac{Lt}{A}\right)\frac{1}{2(1+\sigma)}\frac{4C_2}{\left\{\left(\frac{n\pi}{2}\right)^2+\gamma\right\}} + 2(2LZ_R)\left(\frac{Lt}{A}\right)\left(\frac{a}{b}\right)\frac{\left(\frac{a}{t}-\frac{b}{t_R}\right)}{\left(\frac{a}{t}+\frac{b}{t_R}\right)}\left\{\frac{1}{n^2\pi^2} - \frac{(-)^{(n-1)/2}2}{n^3\pi^3}\right\}$$

and substituting from equation (75), the above becomes

$$\varphi_n A_n - \sum_{m=1}^{\infty}\psi_m A_m = (2LZ_R)\theta_n\,, \qquad \ldots \qquad (76)$$

where m is an odd integer and

$$\varphi_n = (-)^{(n-1)/2}\, n\pi\left\{\left(\frac{n\pi}{2}\right)^2+\gamma\right\}\rho_n\sinh\frac{n\pi\beta^{1/2}}{2}\,,$$

$$\psi_m = (-)^{(m-1)/2}\left(\frac{Lt}{A}\right)\frac{1}{2(1+\sigma)}8\gamma^{1/2}(\nu_m+1)\coth\gamma^{1/2}\sinh\frac{m\pi\beta^{1/2}}{2}$$

$$\theta_n = \frac{\left(\frac{Lt}{A}\right)}{\left(\frac{a}{t}+\frac{b}{t_R}\right)}\left[2\left(\frac{a}{t_R}\right)\gamma^{1/2}\,\mathrm{cosech}\,\gamma^{1/2} - (-)^{(n-1)/2}\left(\frac{a}{t_R}\right)n\pi\right.$$

$$\left.+(-)^{(n-1)/2}\left(\frac{a}{b}\right)\left(\frac{a}{t}-\frac{b}{t_R}\right)\frac{n\pi}{2}\left\{\left(\frac{n\pi}{2}\right)^2+\gamma\right\}\left\{\left(\frac{2}{n\pi}\right)^2 - (-)^{(n-1)/2}\left(\frac{2}{n\pi}\right)^3\right\}\right].$$

Finally, the solution to equations (76) is

$$A_n = \frac{(2LZ_R)}{\varphi_n}\left\{\theta_n + \frac{\sum_{m=1}^{\infty}\frac{\theta_m\psi_m}{\varphi_m}}{1-\sum_{m=1}^{\infty}\frac{\psi_m}{\varphi_m}}\right\} \qquad \ldots \qquad (77)$$

and with these values of A_n the stress distribution may be evaluated throughout the entire wing structure. The z-wise displacement may be evaluated from equations (20) or (64).

The convergence of the series for the stress in the spar booms is of the order $1/n^2$ (*cf.* Appendix IV) if calculated direct from equation (71). The convergence is, however, improved by $1/n$ if the spar boom stress is evaluated from the expression

$$\frac{P}{A} = \frac{E}{L}\frac{\partial u}{\partial\xi}\bigg/_{\eta=1} = -\frac{L}{A}\int_{\xi}^{1}(S_R + S/_{\eta=1})\,d\xi\,. \qquad \ldots \qquad (78)$$

APPENDIX X

The Torsional Case
Numerical Illustrative Example

1. *General.*—The numerical illustrative example is based on the same wing as in Appendix V. The calculations are for a uniformly distributed load $2LZ_R = 1 \cdot 0$ lb along each spar, the loading being anti-symmetrical about the centre line of the wing box.

2. *Numerical Example for Appendix VIII.*—2.1. *Solution Using Only the Functions $F(\xi)$ and $F_1(\xi)$.*—Substituting the numerical values into the differential equations (62) it is found that $F(\xi)$ and $F_1(\xi)$ are determined from

$$1 \cdot 523438 \frac{d^4F}{d\xi^4} - 465 \cdot 8333 \frac{d^2F}{d\xi^2} + 4{,}000F + 0 \cdot 2539062 \frac{d^4F_1}{d\xi^4}$$

$$- 77 \cdot 63889 \frac{d^2F_1}{d\xi^2} + 1{,}333 \cdot 333F_1 = - 2 \cdot 166667 + 66 \cdot 66667(1 - \xi)^2 ,$$

and

$$0 \cdot 2539063 \frac{d^4F}{d\xi^4} - 77 \cdot 63889 \frac{d^2F}{d\xi^2} + 1{,}333 \cdot 333F + 0 \cdot 1144208 \frac{d^4F_1}{d\xi^4}$$

$$- 21 \cdot 17533 \frac{d^2F_1}{d\xi^2} + 609 \cdot 2291F_1 = - 0 \cdot 3611111 + 22 \cdot 22222(1 - \xi)^2 .$$

The solution to these equations may be written

$$\begin{aligned} F(\xi) = {} & C_1 \cosh \gamma_1\xi + C_2 \sinh \gamma_1\xi + C_3 \cosh \gamma_2\xi + C_4 \sinh \gamma_2\xi + C_5 \cosh \alpha\xi \cos \beta\xi \\ & + C_6 \sinh \alpha\xi \cos \beta\xi + C_7 \sinh \alpha\xi \sin \beta\xi + C_8 \cosh \alpha\xi \sin \beta\xi \\ & + 0 \cdot 0166667(1 - \xi)^2 + 0 \cdot 00784485 , \end{aligned}$$

$$\begin{aligned} F_1(\xi) = {} & - 1 \cdot 90397(C_1 \cosh \gamma_1\xi + C_2 \sinh \gamma_1\xi) - 0 \cdot 154776(C_3 \cosh \gamma_2\xi + C_4 \sinh \gamma_2\xi) \\ & + C_5(- 7 \cdot 20628 \cosh \alpha\xi \cos \beta\xi - 0 \cdot 644458 \sinh \alpha\xi \sin \beta\xi) \\ & + C_6(- 7 \cdot 20628 \sinh \alpha\xi \cos \beta\xi - 0 \cdot 644458 \cosh \alpha\xi \sin \beta\xi) \\ & + C_7(- 7 \cdot 20628 \sinh \alpha\xi \sin \beta\xi + 0 \cdot 644458 \cosh \alpha\xi \cos \beta\xi) \\ & + C_8(- 7 \cdot 20628 \cosh \alpha\xi \sin \beta\xi + 0 \cdot 644458 \sinh \alpha\xi \cos \beta\xi) \\ & - 0 \cdot 00135137 \end{aligned}$$

where

$$\gamma_1 = 2 \cdot 16022,$$

$$\gamma_2 = 17 \cdot 2388,$$

$$\alpha = 7 \cdot 90116,$$

$$\beta = 1 \cdot 83074.$$

The arbitrary constants $C_1, C_2, \ldots C_8$ are determined from the boundary conditions given in equation (63) and this results in the following systems of simultaneous equations,

$$\begin{bmatrix} 2\cdot16022 & 17\cdot2388 & 7\cdot90116 & 1\cdot83074 \\ 4\cdot11300 & 2\cdot66815 & 58\cdot1178 & 8\cdot10086 \\ 676\cdot491 & 220\cdot064 & -649\cdot736 & 259\cdot301 \\ 80\cdot2598 & 71\cdot8750 & -356\cdot258 & 132\cdot239 \end{bmatrix} \begin{bmatrix} C_2 \\ C_4 \\ C_6 \\ C_8 \end{bmatrix} = \begin{bmatrix} 0\cdot0333333 \\ 0 \\ 13\cdot3611 \\ 2\cdot22685 \end{bmatrix},$$

which has the solution

$$\begin{aligned} C_2 &= 0\cdot17435 \times 10^{-1}, \\ C_4 &= 0\cdot23384 \times 10^{-3}, \\ C_6 &= -0\cdot15261 \times 10^{-2}, \\ C_8 &= 0\cdot20195 \times 10^{-2}, \end{aligned}$$

and

$$\begin{bmatrix} 4\cdot39419 & 15{,}335{,}200 & -347\cdot037 & 1{,}304\cdot84 \\ 9\cdot24336 & 264{,}360{,}000 & -5{,}130\cdot82 & 9{,}674\cdot41 \\ -8\cdot36641 & -2{,}373{,}510 & 1{,}659\cdot93 & -9{,}626\cdot69 \\ -17\cdot5991 & -40{,}916{,}500 & 30{,}739\cdot4 & -73{,}023\cdot1 \end{bmatrix} \begin{bmatrix} C_1 \\ C_3 + C_4 \\ C_5 + C_6 \\ C_7 + C_8 \end{bmatrix} = \begin{bmatrix} -0\cdot0824461 \\ -0\cdot165498 \\ 0\cdot155552 \\ 0\cdot315103 \end{bmatrix}$$

which has the solution

$$\begin{aligned} C_1 &= -\,0\cdot18945 \times 10^{-1}, \\ C_3 + C_4 &= 0\cdot28826 \times 10^{-10}, \\ C_5 + C_6 &= 0\cdot25939 \times 10^{-6}, \\ C_7 + C_8 &= 0\cdot34373 \times 10^{-6}. \end{aligned}$$

Substituting the above values into the equations of Appendix VIII it is possible to obtain the distorted shape and the stress distribution for the wing structure. The stress distributions are shown in Figs. 18 to 22 and the z-wise displacements of the spar booms are shown in Fig. 23, The rib-web shear stresses are negligibly small and have not been plotted.

2.2. *The Conventional Solution.*—The conventional solution is derived by putting all the $F_n(\xi)$ equal to zero and using an effective boom area A_e where

$$A_e = A + \frac{at^*}{3} = 16\cdot6667 \text{ in.}^2.$$

Substituting the numerical values into equation (67) it is found that $F(\xi)$ is determined from

$$1\cdot523438 \frac{d^4F}{d\xi^4} - 465\cdot8333 \frac{d^2F}{d\xi^2} + 2{,}400F = -\,2\cdot166667 + 40(1 - \xi)^2 .$$

The solution to this equation may be written

$$\begin{aligned} F = {} & C_1 \cosh \gamma_1\xi + C_2 \sinh \gamma_1\xi + C_3 \cosh \gamma_2\xi + C_4 \sinh \gamma_2\xi \\ & + 0\cdot0166667(1 - \xi)^2 + 0\cdot00556713 , \end{aligned}$$

where $\gamma_1 = 2\cdot28952$

$\gamma_2 = 17\cdot3360 .$

The arbitrary constants C_1, C_2, C_3, C_4 are determined from the boundary conditions given in equation (63) and this results in the following systems of simultaneous equations,

$$\begin{bmatrix} 2\cdot 28952 & 17\cdot 3360 \\ 1{,}048\cdot 25 & 138\cdot 440 \end{bmatrix} \begin{bmatrix} C_2 \\ C_4 \end{bmatrix} = \begin{bmatrix} 0\cdot 0333333 \\ 13\cdot 3611 \end{bmatrix},$$

which has the solution

$$C_2 = 0\cdot 12714 \times 10^{-1}$$
$$C_4 = 0\cdot 24369 \times 10^{-3},$$

and

$$\begin{bmatrix} 4\cdot 98578 \\ 11\cdot 1831 \end{bmatrix} \begin{bmatrix} 16{,}900{,}000 \\ 292{,}978{,}000 \end{bmatrix} \begin{bmatrix} C_1 \\ C_3 + C_4 \end{bmatrix} = \begin{bmatrix} -0\cdot 0676677 \\ -0\cdot 142180 \end{bmatrix}$$

which has the solution

$$C_1 = -\ 0\cdot 13661 \times 10^{-1}$$
$$C_3 + C_4 = 0\cdot 26066 \times 10^{-10}.$$

The stress distributions and displacements for this solution are compared with some of those obtained from the first solution in Figs. 18 to 23.

2.3. *The Conventional Solution where the Ribs are Assumed Rigid.*—When the ribs are assumed rigid the thickness of ribs τ per unit run becomes infinite and $F(\xi)$ is then determined from equation (69), *i.e.*,

$$-\ 465\cdot 8333\frac{d^2F}{d\xi^2} + 2{,}400F = -\ 2\cdot 16667 + 40(1-\xi)^2.$$

The solution to this equation may be written

$$F = C_1 \cosh \gamma\xi + C_2 \sinh \gamma\xi + 0\cdot 0166667\ (1-\xi)^2 + 0\cdot 00556713$$

where $\gamma = 2\cdot 26981$.

The arbitrary constants C_1, C_2 are determined from the boundary conditions given in equation (63), whence

$$C_1 = -\ 0\cdot 13508 \times 10^{-1}$$
$$C_2 = 0\cdot 12636 \times 10^{-1}.$$

The stress distributions and displacements for this solution are compared with some of those obtained from the first solution in Figs. 18 to 23.

3. *Numerical Example for Appendix IX.*—The value of the non-dimensional parameter β is $\beta = 0\cdot 866667$, as for the flexural case. The constants A_n are determined from equation (77) and are found to be

$$A_1 = 0\cdot 29720,$$
$$A_3 = 0\cdot 59772 \times 10^{-1},$$
$$A_5 = 0\cdot 54139 \times 10^{-4},$$
$$A_7 = 0\cdot 17154 \times 10^{-5},$$
$$A_9 = 0\cdot 30885 \times 10^{-7},$$
$$A_{11} = 0\cdot 13004 \times 10^{-8},$$
$$A_{13} = 0\cdot 30727 \times 10^{-10},$$
$$A_{15} = 0\cdot 14806 \times 10^{-11}.$$

Using these values, the stress distribution and distorted shape have been calculated and are compared with the results obtained from the method of Appendix VIII in Figs. 18 to 23.

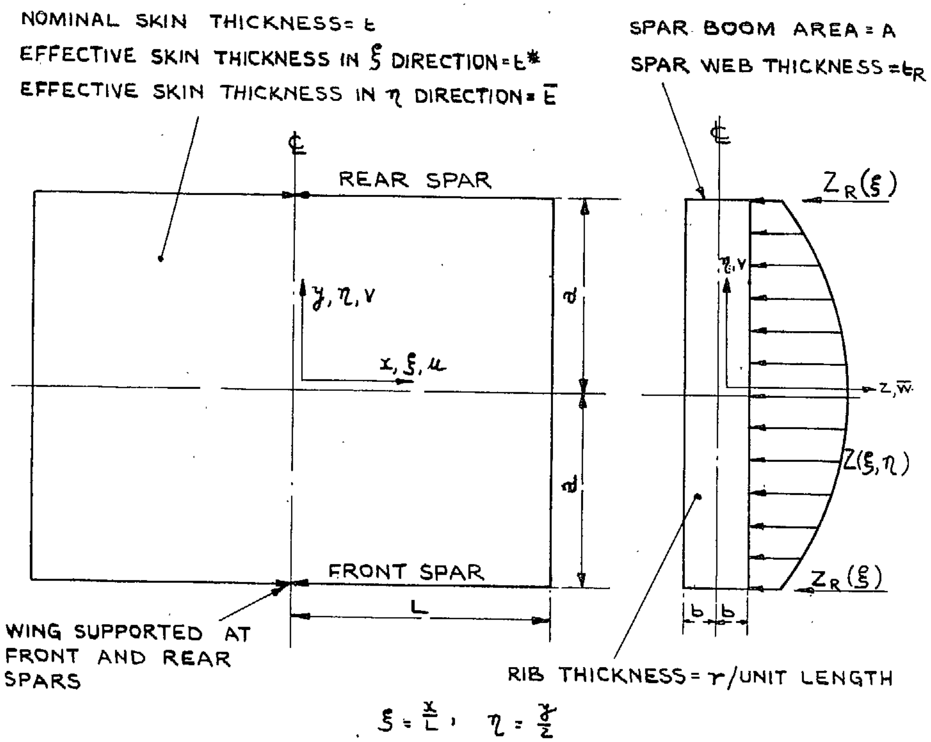

FIG. 1. Notation and co-ordinate system for wing box.

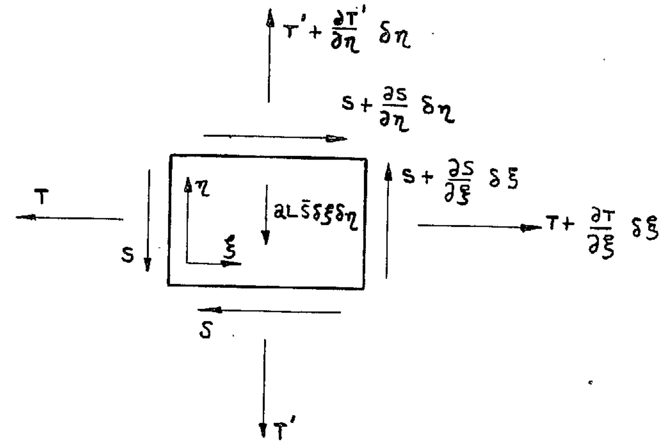

FIG. 2. Stress resultants acting on an elemental portion of the reinforced skin at $z = \pm b$.

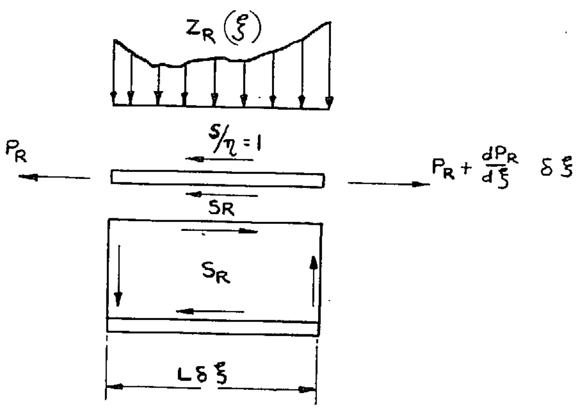

FIG. 3. Forces acting on an elemental portion of the rear spar boom.

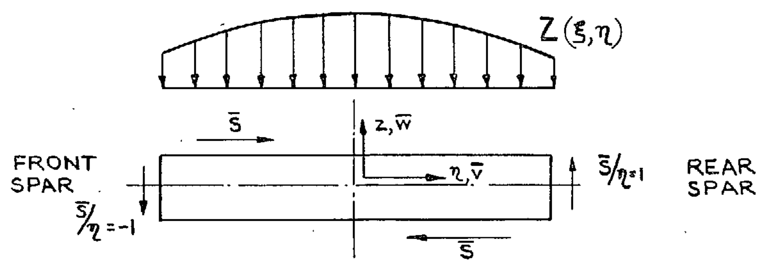

FIG. 4. Forces acting on a rib.

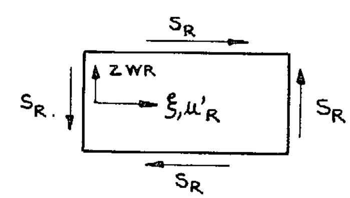

FIG. 5. Forces acting on the rear spar web.

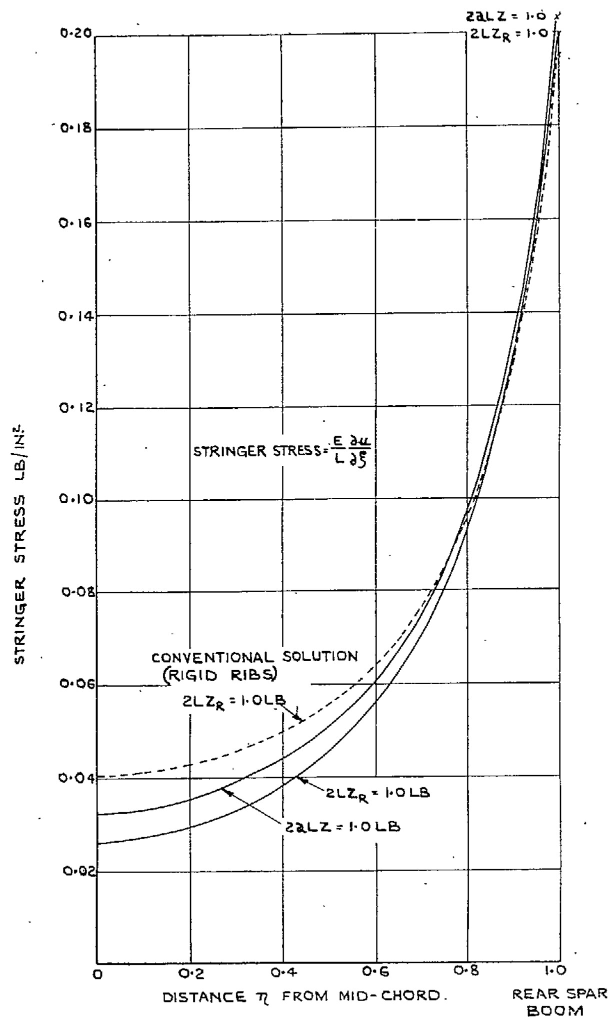

FIG. 6. Flexural Case.—Chordwise distribution of stringer stresses at the root section.

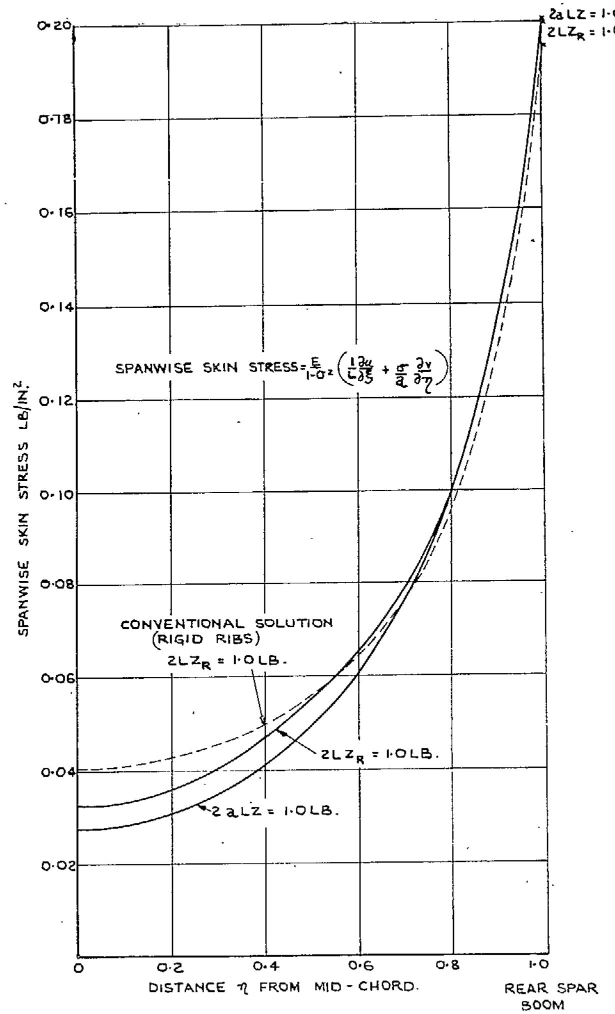

FIG. 7. Flexural Case.—Chordwise distribution of the spanwise skin stresses at the root section.

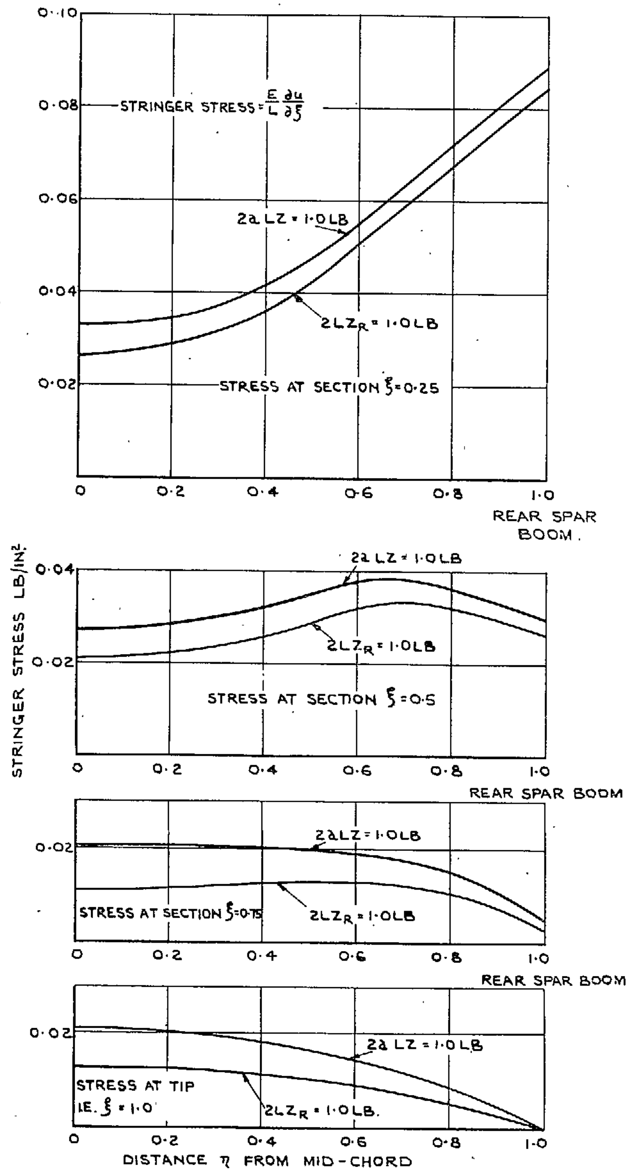

FIG. 8. Flexural Case.—Chordwise distribution of stringer stresses at various sections along the span.

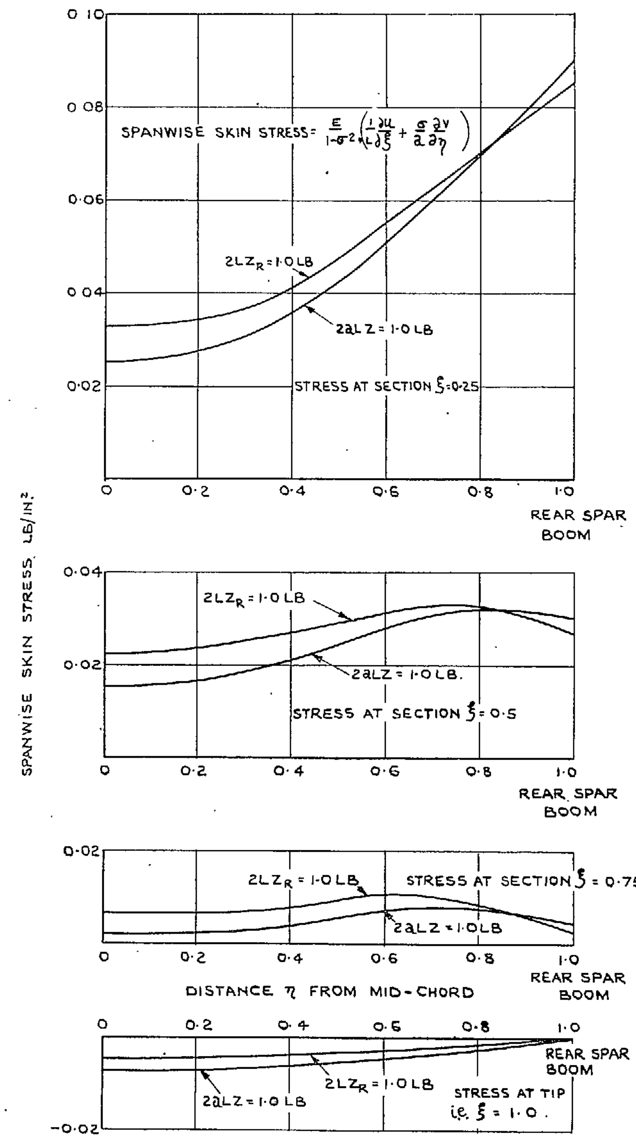

FIG. 9. Flexural Case.—Chordwise distribution of the spanwise skin stresses at various sections along the span.

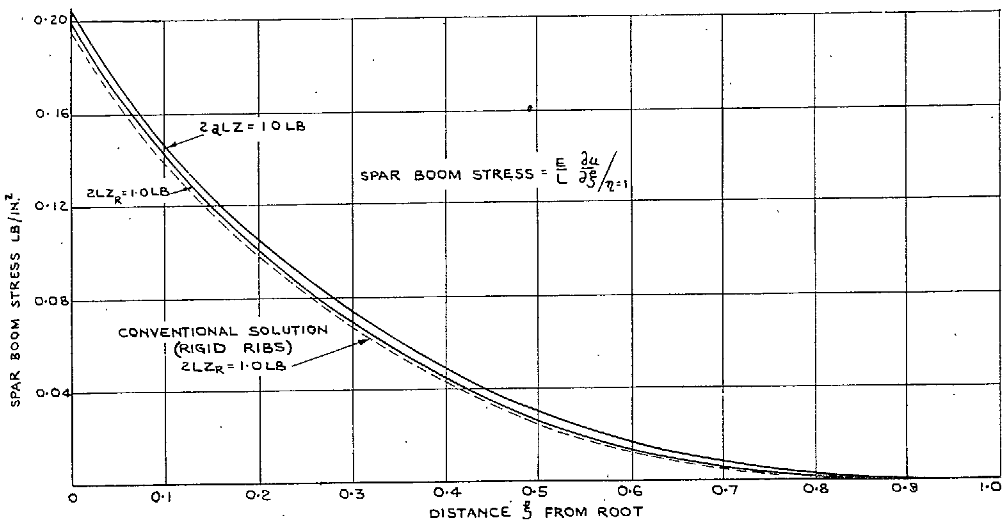

FIG. 10. Flexural Case.—Spanwise distribution of spar-boom stresses.

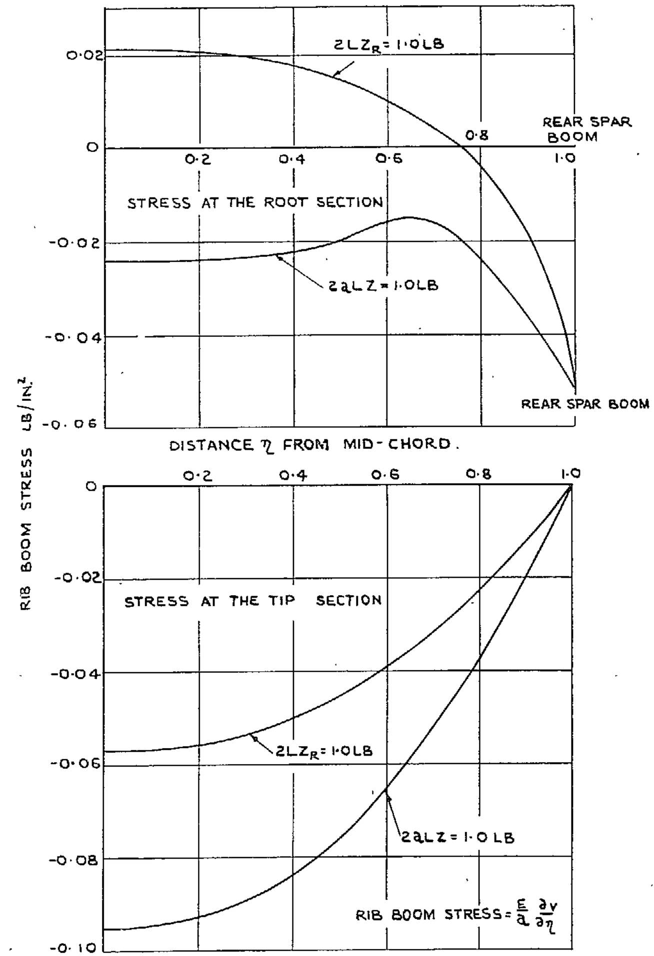

FIG. 11. Flexural Case.—Chordwise distribution of rib-boom stresses at the root and tip sections.

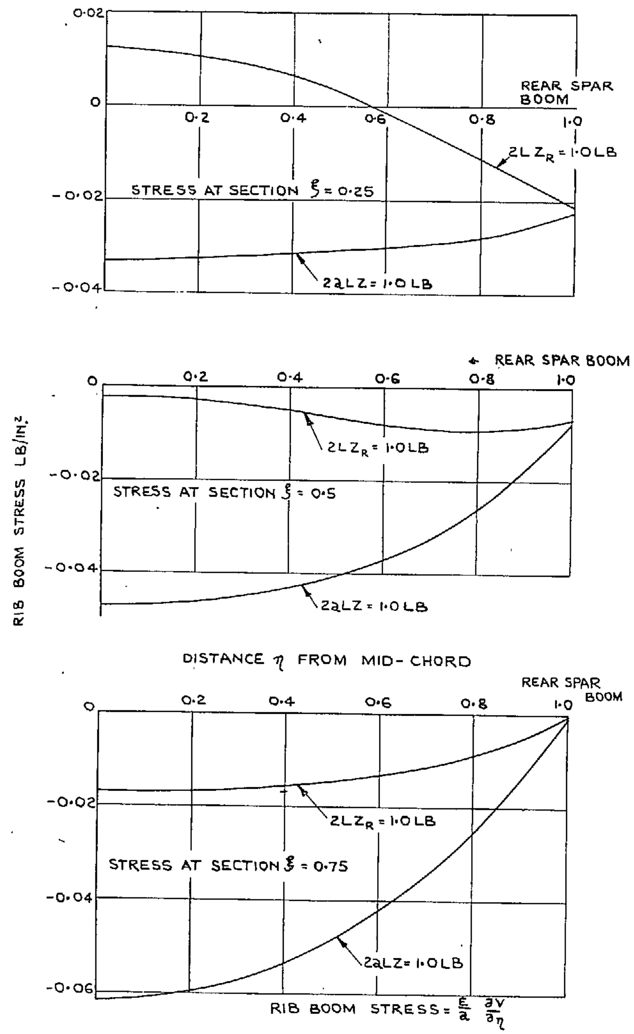

FIG. 12. Flexural Case.—Chordwise distribution of rib-boom stresses at various sections along the span.

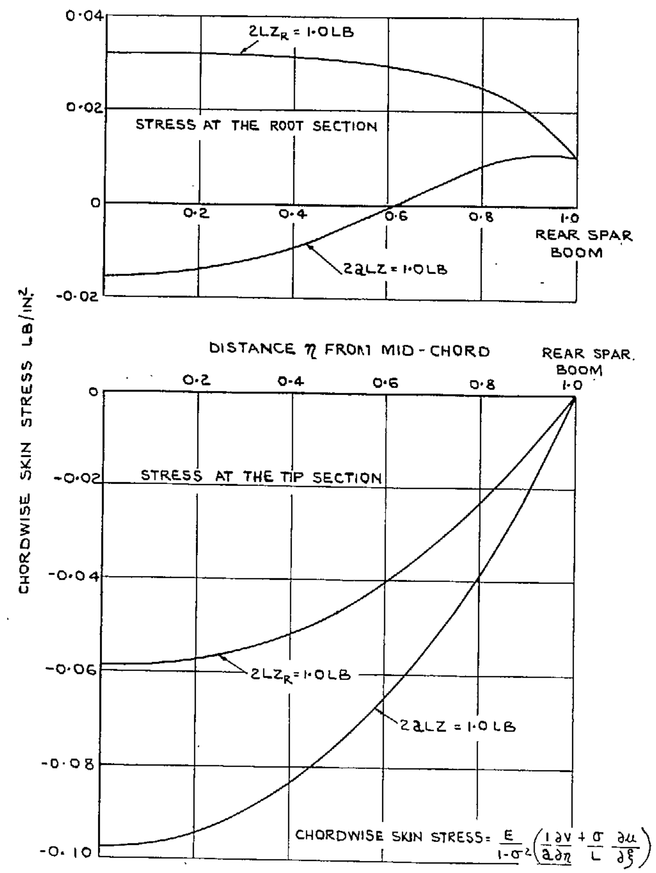

FIG. 13. Flexural Case.—Chordwise distribution of the chordwise skin stresses at the root and tip sections.

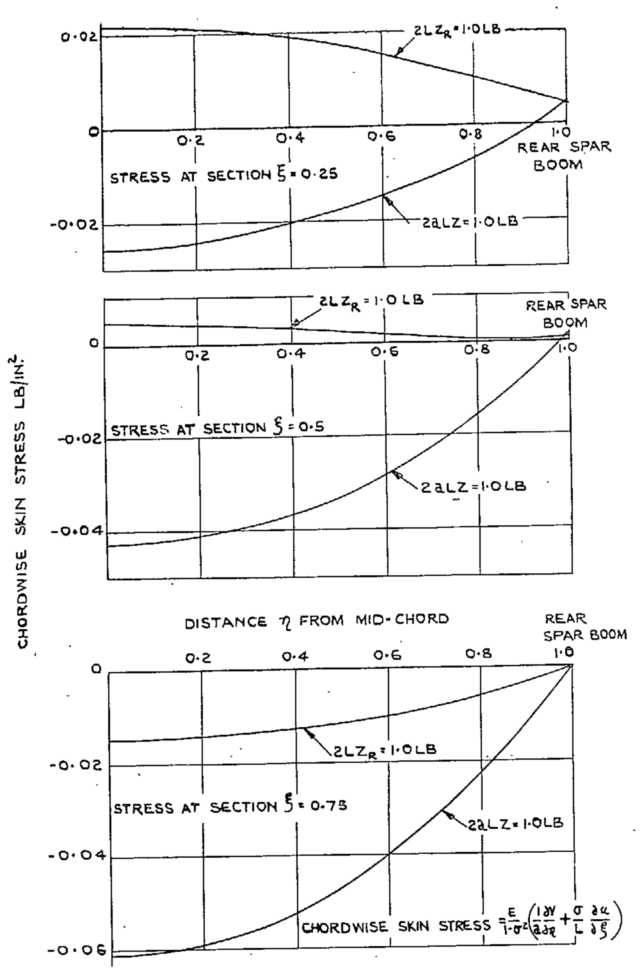

FIG. 14. Flexural Case.—Chordwise distribution of the chordwise skin stresses at various sections along the span.

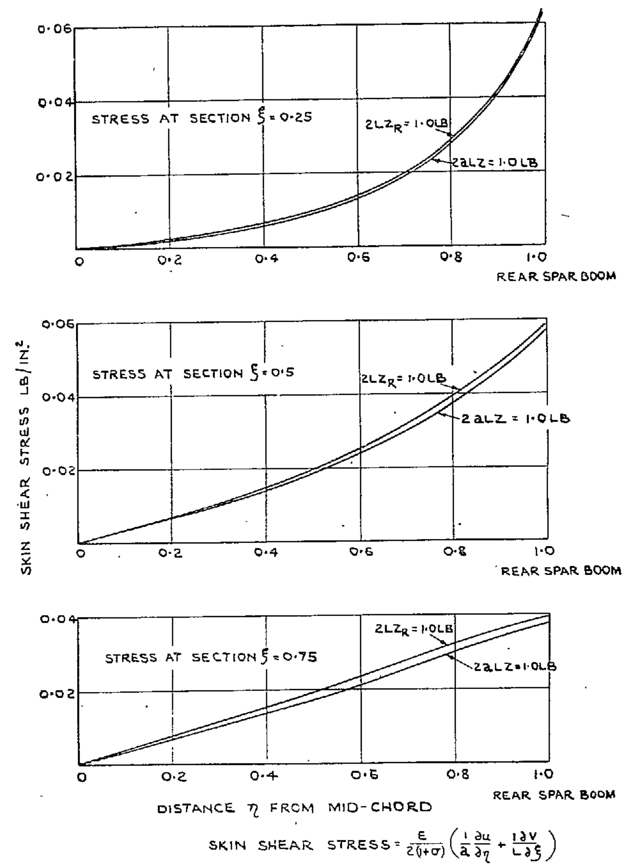

FIG. 15. Flexural Case.—Chordwise distribution of the skin shear stresses at various sections along the span.

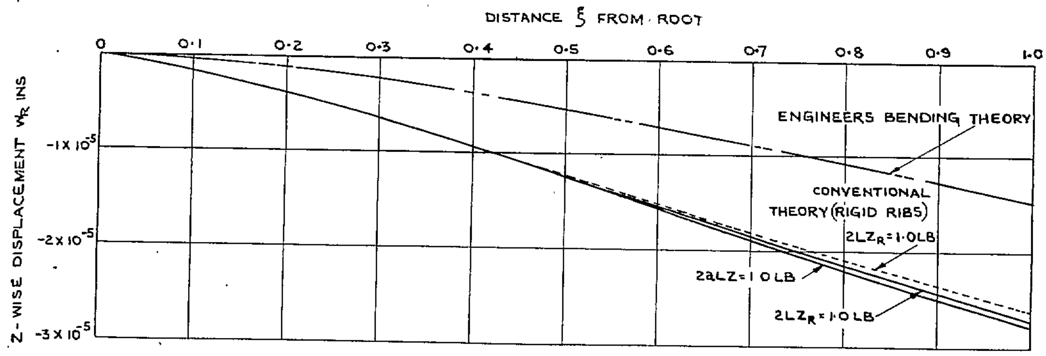

FIG. 16. Flexural Case.—z-wise displacements of the spar booms.

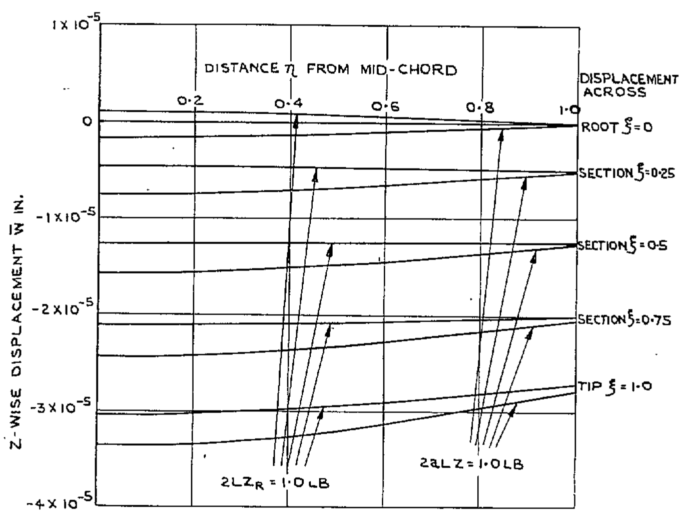

FIG. 17. Flexural Case.—z-wise displacements along a chord at various sections along the span.

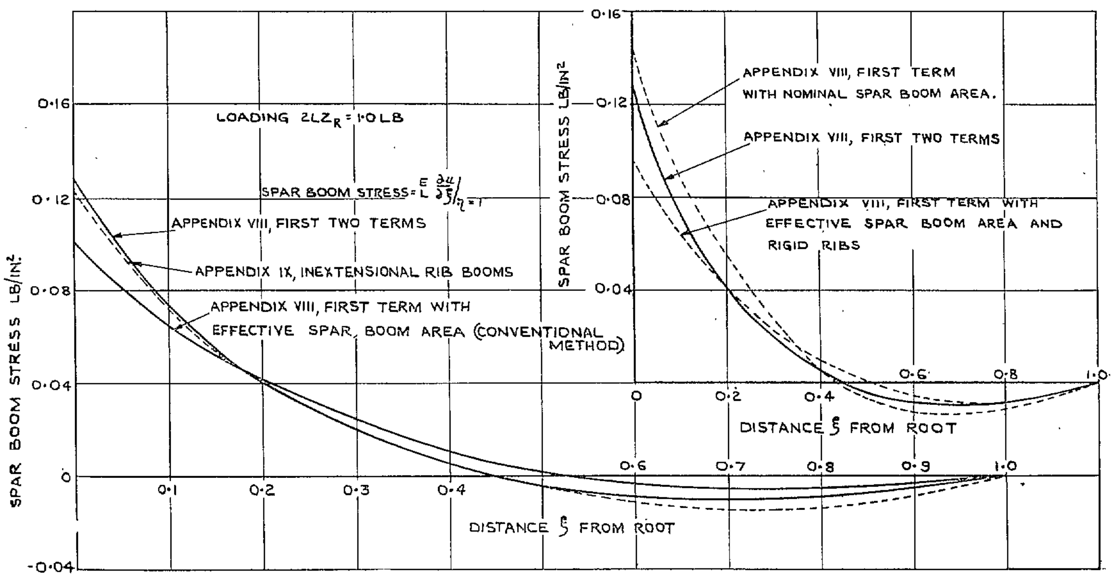

Fig. 18. Torsional Case.—Spanwise distribution of spar-boom stress.

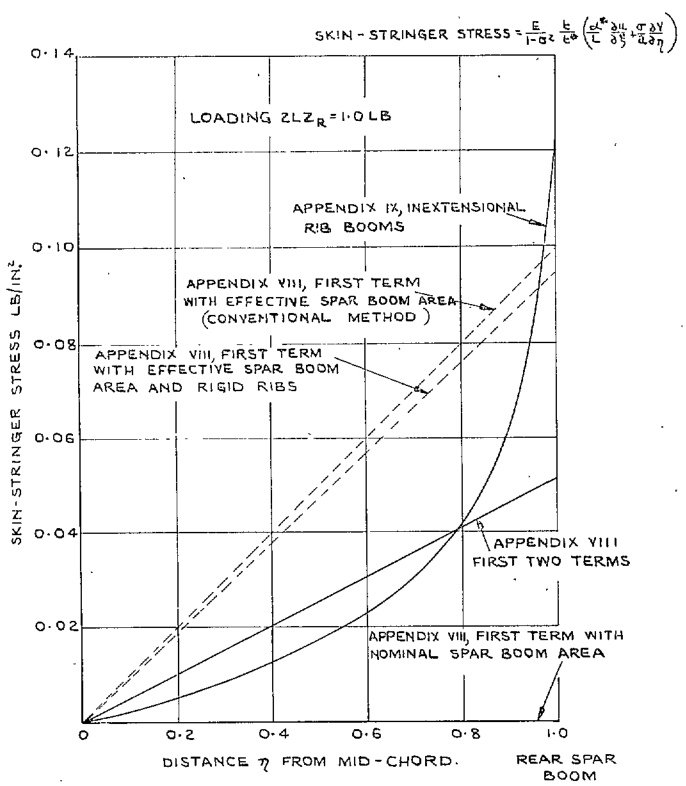

Fig. 19. Torsional Case.—Chordwise distribution of the skin-stringer stresses at the root.

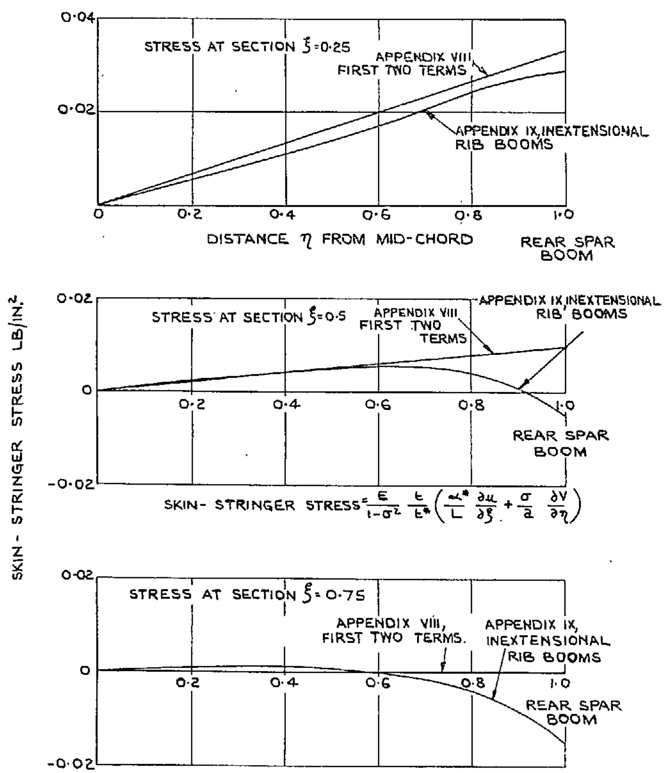

FIG. 20. Torsional Case.—Chordwise distribution of the skin-stringer stresses at various sections along the span.

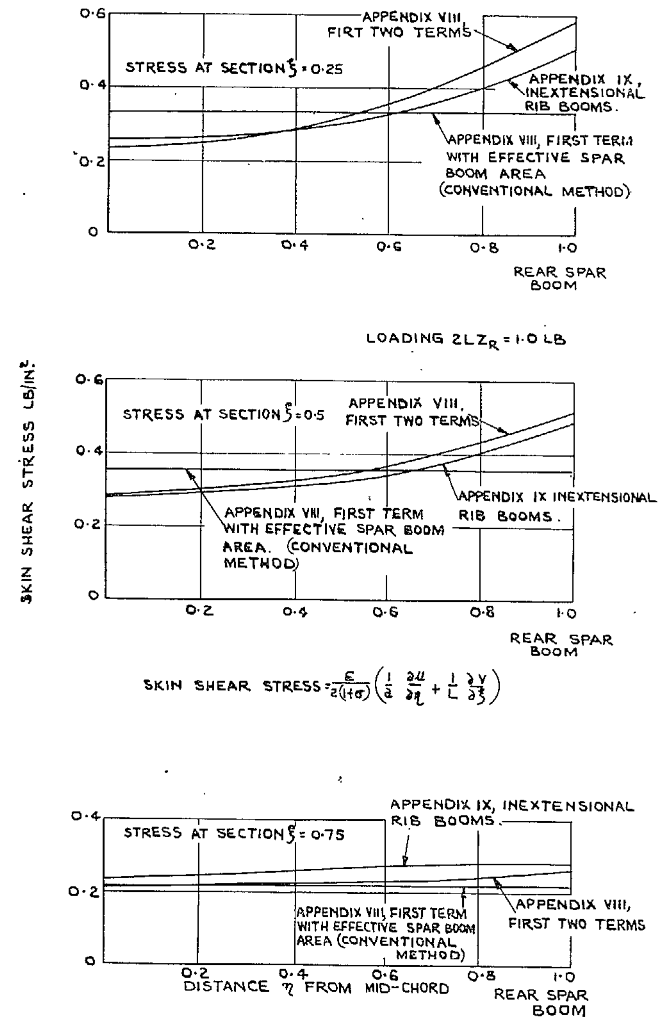

FIG. 21. Torsional Case.—Chordwise distribution of the skin shear stresses at various sections along the span.

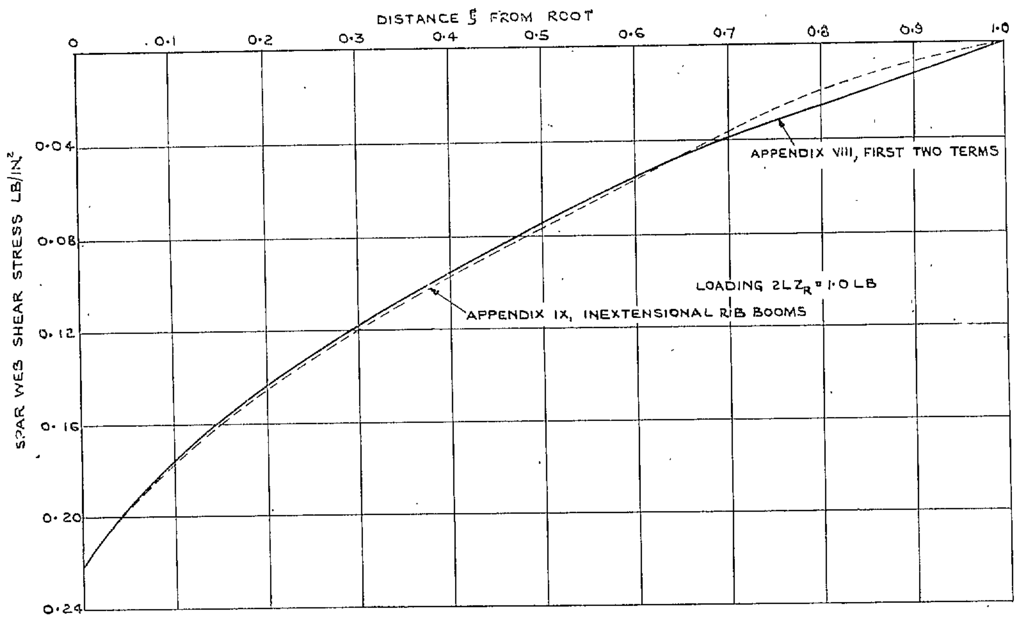

FIG. 22. Torsional Case.—Spanwise distribution of spar-web shear stresses.

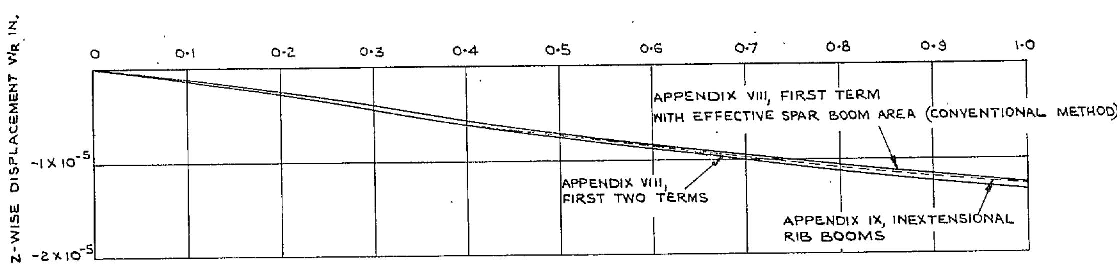

FIG. 23. Torsional Case. z-wise displacements of the spar booms.

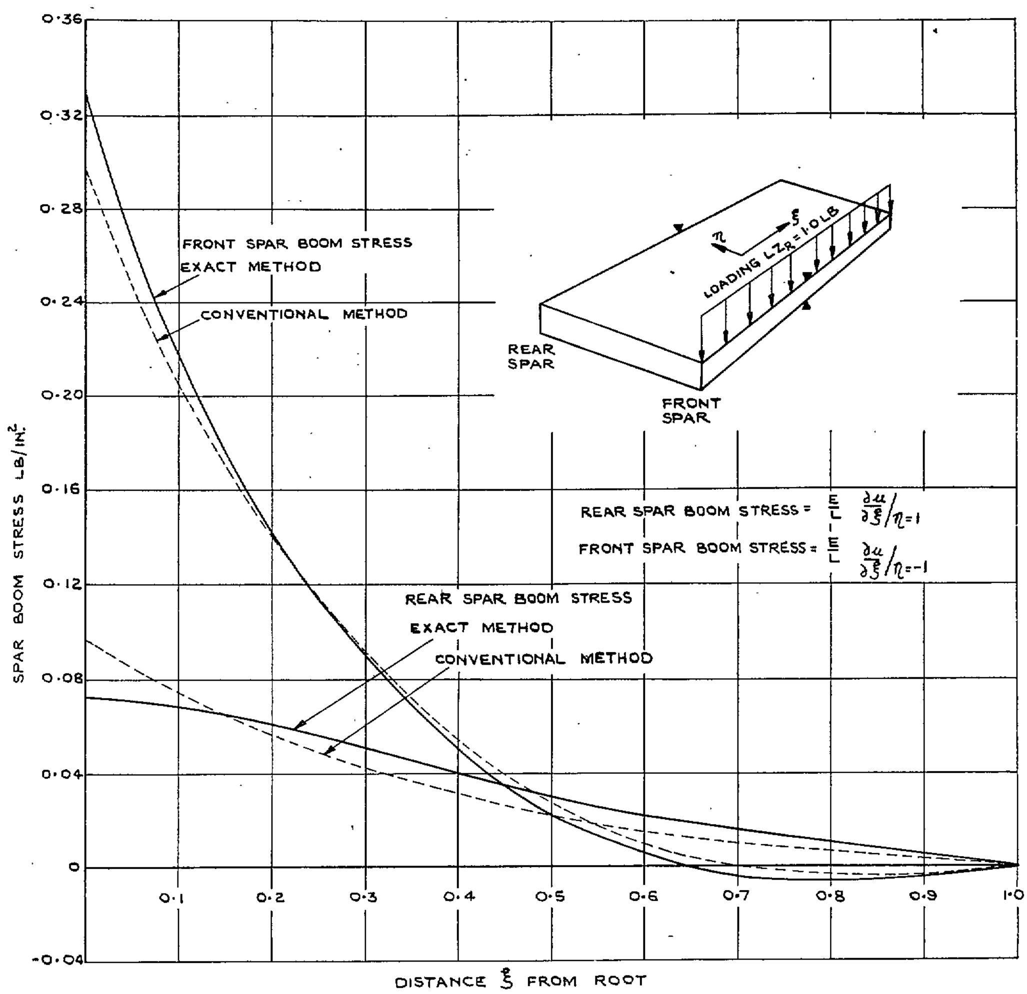

FIG. 24. Loading along one spar.—Spanwise distribution of spar-boom stresses.

J4384 52/8943 K7 7/57 D&Co. 34/263

PRINTED IN GREAT BRITAIN

D

Publications of the Aeronautical Research Council

ANNUAL TECHNICAL REPORTS OF THE AERONAUTICAL RESEARCH COUNCIL (BOUND VOLUMES)

1939 Vol. I. Aerodynamics General, Performance, Airscrews, Engines. 50s. (52s.)
Vol. II. Stability and Control, Flutter and Vibration, Instruments, Structures, Seaplanes, etc. 63s. (65s.)

1940 Aero and Hydrodynamics, Aerofoils, Airscrews, Engines, Flutter, Icing, Stability and Control, Structures, and a miscellaneous section. 50s. (52s.)

1941 Aero and Hydrodynamics, Aerofoils, Airscrews, Engines, Flutter, Stability and Control, Structures. 63s. (65s.)

1942 Vol. I. Aero and Hydrodynamics, Aerofoils, Airscrews, Engines. 75s. (77s.)
Vol. II. Noise, Parachutes, Stability and Control, Structures, Vibration, Wind Tunnels. 47s. 6d. (49s. 6d.)

1943 Vol. I. Aerodynamics, Aerofoils, Airscrews. 80s. (82s.)
Vol. II. Engines, Flutter, Materials, Parachutes, Performance, Stability and Control, Structures. 90s. (92s. 9d.)

1944 Vol. I. Aero and Hydrodynamics, Aerofoils, Aircraft, Airscrews, Controls. 84s. (86s. 6d.)
Vol. II. Flutter and Vibration, Materials, Miscellaneous, Navigation, Parachutes, Performance, Plates and Panels, Stability, Structures, Test Equipment, Wind Tunnels. 84s. (86s. 6d.)

1945 Vol. I. Aero and Hydrodynamics, Aerofoils. 130s. (132s. 9d.)
Vol. II. Aircraft, Airscrews, Controls. 130s. (132s. 9d.)
Vol. III. Flutter and Vibration, Instruments, Miscellaneous, Parachutes, Plates and Panels, Propulsion. 130s (132s. 6d.)
Vol. IV. Stability, Structures, Wind tunnels, Wind Tunnel Technique. 130s. (132s. 6d.)

ANNUAL REPORTS OF THE AERONAUTICAL RESEARCH COUNCIL—

1937 2s. (2s. 2d.) 1938 1s. 6d. (1s. 8d.) 1939–48 3s. (3s. 5d.)

INDEX TO ALL REPORTS AND MEMORANDA PUBLISHED IN THE ANNUAL TECHNICAL REPORTS, AND SEPARATELY—

April, 1950 - - - - - R. & M. No. 2600. 2s. 6d. (2s. 10d.)

AUTHOR INDEX TO ALL REPORTS AND MEMORANDA OF THE AERONAUTICAL RESEARCH COUNCIL—

1909–January, 1954 - - - R. & M. No. 2570. 15s. (15s. 8d.)

INDEXES TO THE TECHNICAL REPORTS OF THE AERONAUTICAL RESEARCH COUNCIL—

December 1, 1936 — June 30, 1939.	R. & M. No. 1850.	1s. 3d. (1s. 5d.)
July 1, 1939 — June 30, 1945. -	R. & M. No. 1950.	1s. (1s. 2d.)
July 1, 1945 — June 30, 1946. -	R. & M. No. 2050.	1s. (1s. 2d.)
July 1, 1946 — December 31, 1946.	R. & M. No. 2150.	1s. 3d. (1s. 5d.)
January 1, 1947 — June 30, 1947. -	R. & M. No. 2250.	1s. 3d. (1s. 5d.)

PUBLISHED REPORTS AND MEMORANDA OF THE AERONAUTICAL RESEARCH COUNCIL—

Between Nos. 2251–2349. - -	R. & M. No. 2350.	1s. 9d. (1s. 11d.)
Between Nos. 2351–2449. - -	R. & M. No. 2450.	2s. (2s. 2d.)
Between Nos. 2451–2549. - -	R. & M. No. 2550.	2s. 6d. (2s. 10d.)
Between Nos. 2551–2649. - -	R. & M. No. 2650.	2s. 6d. (2s. 10d.)
Between Nos. 2651–2749. - -	R. & M. No. 5750.	2s. 6d. (2s. 10d.)

Prices in brackets include postage

HER MAJESTY'S STATIONERY OFFICE

York House, Kingsway, London W.C.2; 423 Oxford Street, London W.1; 13a Castle Street, Edinburgh 2; 39 King Street, Manchester 2; 2 Edmund Street, Birmingham 3; 109 St. Mary Street, Cardiff; Tower Lane, Bristol 1; 80 Chichester Street, Belfast, *or through any bookseller*

S.O. Code No. 23-3052

R. & M. No. 3052